Interpretation of the vibrational energy level structure of the astructural molecular ion H5+ and all of its deuterated isotopomers

János Sarka and Attila G. Császár

Citation: The Journal of Chemical Physics **144**, 154309 (2016); doi: 10.1063/1.4946808
View online: http://dx.doi.org/10.1063/1.4946808
View Table of Contents: http://scitation.aip.org/content/aip/journal/jcp/144/15?ver=pdfcov
Published by the AIP Publishing

Interpretation of the vibrational energy level structure of the astructural molecular ion H_5^+ and all of its deuterated isotopomers

János Sarka[1,2] and Attila G. Császár[1,2,a)]
[1]*Laboratory of Molecular Structure and Dynamics, Institute of Chemistry, Eötvös University, Pázmány Péter sétány 1/A, H-1117 Budapest, Hungary*
[2]*MTA-ELTE Complex Chemical Systems Research Group, P.O. Box 32, H-1518 Budapest 112, Hungary*

(Received 28 November 2015; accepted 4 April 2016; published online 20 April 2016)

Variational nuclear motion computations, employing an exact kinetic energy operator and two different potential energy surfaces, are performed to study the first 60 vibrational states of the molecular ion $H_5^+ \equiv [H_2–H–H_2]^+$ and all of its deuterated isotopologues and isotopomers, altogether 12 species. Detailed investigation of the vibrational wavefunctions mostly results in physically intuitive labels not only for the fundamentals but also for the overtone and combination states computed. The torsional motion associated with the left and right diatomics appears to be well separated from the other vibrational degrees of freedom for all species. The unusual structure of the higher-lying bending states and the heavy mixing of the internal motions is partly due to the astructural character of all these molecular ions. The existence of distinct isotopomers in the $H_{5-n}D_n^+$, $n = 1$–4 cases, in the energy range studied, is confirmed. Two rules determine the stability order of the isotopomers: first, when possible, H prefers to stay in the middle of the ions rather than at the sides, and, second, the isotopomer with a homonuclear diatomic at the side is always lower in energy. The large number of precise vibrational energies of the present study, as well as the detailed assignment of the states, should serve as benchmarks for future studies by more approximate nuclear-motion treatments, such as diffusion Monte Carlo and multiconfiguration time-dependent Hartree. *Published by AIP Publishing.* [http://dx.doi.org/10.1063/1.4946808]

I. INTRODUCTION

The structure and the low-energy rovibrational dynamics of semirigid molecules can conveniently be characterized using standard tools of quantum chemistry: the harmonic oscillator (HO)[1] and the rigid rotor (RR)[2] models. At the same time, a considerable challenge, even in the fourth age[3] of quantum chemistry, concerns the description of astructural molecules,[4–10] where the RRHO approximation fails to provide even a proper zeroth-order characterization of the structure and the dynamics. The atomic cluster ions H_n^+,[11–13] with $n \geq 5$, form an important class of astructural molecules. As far as stability is considered, similar to most clusters, there are favorite or "magic" n values, the first magic number for H_n^+ is apparently $n = 9$, with the well-bound semirigid molecule H_3^+[14,15] forming the core of the cluster and the core is solvated by three loosely attached H_2 molecules.

The molecular ion H_5^+ is the first important astructural molecule in the H_n^+ family. The unusual structural and dynamical behavior is due to the absence of a "heavy" central atom, the light mass of the whole system, and the existence of several large-amplitude motions hindered by small barriers allowing facile permutation of most of the atoms, which together cause the loss of a well-defined equilibrium structure for H_5^+ and the deuterated $H_nD_{5-n}^+$, $n = 0, 1, 2, 3, 4$ systems. To understand the structure, the rovibrational dynamics, and the related spectra of a system like H_5^+, it is indispensable to use sophisticated quantum chemical tools.[3,16–18] The challenge, the proper and detailed description of these ions of considerable astrochemical and astrophysical interest[13] requires the use of techniques at the forefront of quantum chemistry.

The potential energy surface (PES) of the lowest electronic state of the four-electron H_5^+ molecular ion has been studied via advanced electronic structure techniques.[19–22] Following earlier studies concentrating on the stationary points on the PES,[19] two (semi)global *ab initio* Born–Oppenheimer PES have been developed for the H_5^+ molecule. The first one, hereafter called the XBB PES, was developed by Xie *et al.*[20] based on more than 100 000 carefully chosen CCSD(T)/aug-cc-pVTZ *ab initio* energy points. The second PES, developed by Aguado *et al.*,[21,22] and called hereafter the ABPDVR PES, is built upon more than 110 000 CCSD(T)/aug-cc-pVQZ *ab initio* points and uses the triatoms-in-molecules method to increase the overall accuracy of the fitting procedure. Both PESs display permutational invariance.

During the last decade, based partially on the relatively accurate (semi)global *ab initio* PES available,[20,21] a number of theoretical[7,8,22–36] and experimental[37,38] studies were carried out to characterize the vibrational dynamics of the H_5^+ molecular ion as well as some of its deuterated isotopologues.

Acioli *et al.*[23] performed diffusion Monte Carlo (DMC) computations to determine zero-point vibrational energies (ZPVEs) for H_5^+ and all of its deuterated isotopologues. They found that H prefers to be in the middle rather than

a)Electronic mail: csaszar@chem.elte.hu

at the sides; this results in lower ZPVEs and thus more stable isotopomers. Furthermore, they determined that the zero-point-averaged effective structure of H_5^+ has D_{2d} point-group symmetry. Thus, in the vibrational ground state the $H_5^+ \equiv [H_2–H–H_2]^+$ cation does not differentiate, unlike in its equilibrium structure, between the two H_2 units, left and right of the middle proton. Such a considerable qualitative difference between an equilibrium and an effective ground-state structure is known only in a few other cases, like the CONH "peptide" linkage.[39]

Lin and McCoy[29] computed the ZPVE and a few vibrational states of H_5^+ and D_5^+ using the DMC technique and provided alternative assignments for the measured spectra.[37,38] They confirmed that, although the minimum-energy structure has C_{2v} point-group symmetry, the ground-state probability distribution is delocalized over the two equivalent minima, resulting in an effective structure of D_{2d} point-group symmetry. Later, they extended their study[30] to all possible isotopomers of H_5^+, computed all of the related ZPVEs, and confirmed the energy order of the isotopomers. They also computed the frequency of the internal proton motion ("hopping") for some of the isotopomers. Even later, Lin and McCoy discussed[34] how the large-amplitude motions influence the exchange of the five hydrogen atoms and performed adiabatic DMC computations. They found that the minimum separation of the centers of mass of the H_3^+ and H_2 units is 2.5 Å, where the five hydrogens are free to exchange, increasing the molecular symmetry of the system. In their most recent study, Lin and McCoy[36] also included the effect of deuteration and found that it reduces the amplitude of the wave function close to the transition-state of the proton scrambling.

de Tudela *et al.*[24] and Barragán *et al.*[25] performed classical and path integral Monte Carlo, CMC and PIMC, respectively, computations at 10 K and identified the two most relevant large-amplitude motions of H_5^+: "the H_5^+ probability density distributions show a free intermolecular transfer of the central proton between the two H_2 molecules, which are almost freely rotating around the C_2 axis of H_5^+."[24]

The first determination of a considerable number of vibrational energy levels of H_5^+ is due to Valdes *et al.*,[27] who used the multi-configuration time-dependent Hartree (MCTDH) approach[18,40] to compute the 20 lowest-energy vibrational levels. Later, they extended their study[28] to D_5^+ and used both the XBB and the ABPDVR PESs. They confirmed the ZPVEs of Acioli *et al.*[23] for all of the possible isotopologues and isotopomers. Song *et al.*[31] also computed the first 10 "benchmark" vibrational energy levels of H_5^+ using "full-dimensional quantum calculations"[31] and basically confirmed the assignments provided by Valdes *et al.*[27]

Recently, Valdes and Prosmiti[32] also performed reduced-dimensional (4D) computations to assign the measured experimental infrared spectra[37,38] of H_5^+ and D_5^+ in between 300 and 4500 cm^{-1}. Only the proton-hopping fundamental, ν_{PH}, and its combination bands with the dissociative mode, ν_D, appear in the measured spectra below the first dissociation energy limit, while the H–H stretchings appear above it. Therefore, Valdes and Prosmiti[32] used the R, r_1, r_2, and z coordinates in their 4D model (see Table I and Figure 1). In a set of extensive computations of somewhat limited accuracy, Valdes and Prosmiti,[33] utilizing the MCTDH approach,[18,40] determined 120 selected eigenstates based on full-dimensional computations. They provided labels and wave functions for some of the bending motions and determined the eigenvalue of the internal H_3^+ rotation (the scrambling motion).

McGuire *et al.*[26] investigated the interesting question whether H_5^+ and its deuterated isotopologues would have pure rotational spectra. They determined that the zero-point averaged dipole moments of H_5^+, D_5^+, and HD_4^+ are zero; thus, these ions are not expected to have a pure rotational spectrum. The lack of a dipole moment is due to the effective D_{2d} structure of these ions and the fact that H prefers to be in the center of the ion in case of HD_4^+. According to McGuire *et al.*,[26] the other three deuterated isotopologues, with one, two, and

TABLE I. The internal coordinates and the basis sets employed during the final variational computations of this study; the equilibrium reference geometries and the grid ranges are given in bohr and degrees for the distance- and angle-type coordinates, respectively. The internal coordinates are defined in Figure 1.[a]

			Reference structure[b]				
			ABPDVR[21] PES		XBB[20] PES		
Coord.	DVR type	NBF	C_{2v}	D_{2d}	C_{2v}	D_{2d}	Allowed grid range[c]
R	Laguerre PO-DVR	14	4.0972	4.0972	4.1046	4.104 6	2.5–6.5
r_1	Laguerre PO-DVR	6	1.4504	1.4914	1.4526	1.493 05	0.5–2.5
r_2	Laguerre PO-DVR	6	1.5324	1.4914	1.5335	1.493 05	0.5–2.5
θ_1	Legendre PO-DVR	7	90.0	90.0	90.0	90.0	1.0–179.0
θ_2	Legendre PO-DVR	7	90.0	90.0	90.0	90.0	1.0–179.0
ϕ	Exponential DVR	11	90.0	90.0	90.0	90.0	0.0–360.0
x	Hermite PO-DVR	6	0.0	0.0	0.0	0.0	−1.6 to +1.6
y	Hermite PO-DVR	6	0.0	0.0	0.0	0.0	−1.6 to +1.6
z	Hermite DVR	20	0.3416	0.0	0.3506	0.0	−2.2 to +2.2

[a]Coord. = coordinate, DVR = discrete variable representation, NBF = number of basis functions, PO = potential optimized.
[b]There are computations carried out in this study using either the C_{2v} or the D_{2d} reference structure. Note that the equilibrium structure of H_5^+ has C_{2v} point-group symmetry.
[c]Due to the use of PO-DVR, there can be differences between the allowed and the actual grid ranges for the different isotopomers.

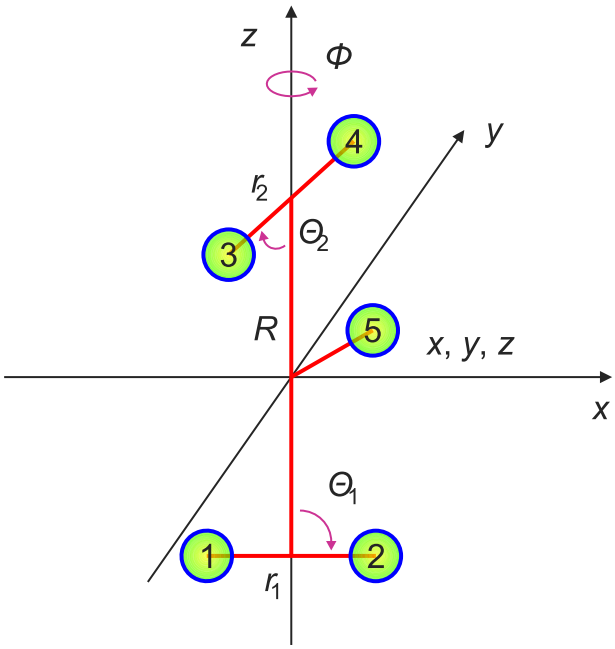

FIG. 1. Internal coordinates of H_5^+ employed in this study.

three Ds are characterized by nonzero dipole moments and thus they could exhibit pure rotational spectra. For these three isotopologues they predicted rotational spectra up to 3 THz. The rotational energy levels utilized differ substantially from those of later, more elaborate studies.[8,35]

Previous efforts[7,8] in our laboratory were carried out to compute and understand the rotational-vibrational energy level structure of H_5^+. The computations showed that H_5^+ has a peculiar rotational-vibrational energy level structure, classifying this molecule as a prototypical astructural molecule. Marlett *et al.*[35] confirmed this assessment and extended the DMC computations to rovibrational states of D_5^+, H_4D^+, and HD_4^+.

As to experiments, in 2010 Cheng *et al.*[37] reported experimental infrared spectra in the 2000–4500 cm^{-1} region. Two years later, basically the same authors[38] extended their study to the mid- and far-IR regions and measured multiple-photon dissociation spectra between 300 and 2200 cm^{-1} using a free-electron laser. They attempted to explain their experimental results using the Reaction Path Hamiltonian version of the code MULTIMODE.[18]

In this work, nuclear motion computations are carried out for the vibrational states of all possible deuterated isotopologues of H_5^+. One of the interesting questions is how many distinct isotopomers exist for the different isotopologues of H_5^+ at different internal excitation energies. This question was asked[23,30] before for the lowest states of the species. It is also important to establish whether the two available PESs[20,21] would result in highly similar or somewhat different vibrational states, as the related results available in the literature based on different approximate solutions of the time-independent nuclear Schrödinger equation show some ambiguity in this respect. Another question concerns the vibrational energy level structure of the isotopologues and isotopomers and whether they can be interpreted based on the computed wavefunctions. It is also of general interest to observe how a substitution by the much heavier D atom affects the internal dynamics of these molecules, with emphasis on the much hindered tunneling along some of the modes. It is also relevant to ask whether any general characteristics could be observed for the energy level sets of the isotopomers studied. Finally, we note that the benchmark-quality results of the present study should also provide important insight into the accuracy of advanced DMC and MCTDH methods in case they are applied for molecules where the approaches useful for semirigid molecules are expected to struggle to yield accurate results.

II. COMPUTATIONAL DETAILS

A. GENIUSH

The full- and the reduced-dimensional nuclear motion computations performed on H_5^+ and its deuterated isotopomers as part of this study utilize the fourth-age[3] quantum chemical algorithm and code GENIUSH.[41–43] The acronym GENIUSH stands for general (GE) rovibrational code with numerical (N), internal-coordinate (I), user-specified (US) Hamiltonians (H). In GENIUSH, the Hamiltonian is written in curvilinear internal coordinates and the representations of both the kinetic and the potential energy operators are computed numerically, utilizing the discrete variable representation (DVR).[44] Computation of the required eigenstates is carried out using different implementations of the iterative Lanczos algorithm.[45]

Characterization of the vibrational states utilizes the node-counting technique, paying attention to the special case of the ϕ coordinate. Several two-dimensional (2D) cuts of the full-dimensional wavefunctions are produced, fixing the seven inactive coordinates at a single value, mostly parameters corresponding to the D_{2d} structure (see Table I for details). Although the node-counting technique works rather well for the lower-energy vibrational states of simple semirigid molecules, for H_5^+ and its isotopomers the different 2D cuts occasionally result in conflicting labels. This can be explained with (a) the lack of a well-defined equilibrium structure to freeze the coordinates to, and (b) the extensive mixing of the vibrational eigenstates.

The masses of the nuclei used during the GENIUSH computations are m_H = 1.007 825 u and m_D = 2.014 102 u.

B. Coordinates

Within the GENIUSH approach the choice of the internal coordinates is of prime importance as convergence of the solution of the nuclear Schödinger equation greatly depends on them and the associated basis functions. In our previous work,[7] several internal coordinate sets were tested for H_5^+ and one of them appeared to be more appropriate than the others. This set of internal coordinates, also applied in this study (see Figure 1 and Table I), was developed by Valdes *et al.*,[27,28] and contains two coordinates for the stretching vectors of the two H_2 units, a stretching coordinate vector between the midpoints of the two H_2 vectors, two bending

coordinates of the two H_2 units regarding the midpoint vector, a torsional coordinate of the two H_2 units, and three Cartesian coordinates to describe the three-dimensional motion of the central hydrogen. (Note that for the two bending coordinates the cosines of the angles mentioned are the effectively used coordinates due to the nature of the Legendre-DVR basis set.) To define the orientation of the molecule, geometric embedding (GE) was employed (see Figure 1 of Ref. 8).

In order to understand the vibrational dynamics of H_5^+, it is important to be able to set up and treat reduced-dimensional models with relative ease. This facility is readily provided by the GENIUSH approach,[41] though it does not work as well for the astructural $H_nD_{5-n}^+$, $n = 0,1,2,3,4,5$ species as for more rigid systems.[7] If all vibrational degrees of freedom are active, the results should not depend on the choice of the internal coordinates. However, for reduced-dimensional computations the choice of the active coordinates becomes a particularly important issue: it is relevant how the constrained coordinates, representing constrained motions, are treated. In this work, mainly during the 1D computations, no relaxation is allowed for the inactive degrees of freedom, the inactive coordinates are always fixed at a single value (see Table I for details).

C. Potential energy surfaces

Both the XBB[20] and the ABPDVR[21] Born–Oppenheimer PESs are characterized by 10 stationary points relevant for the low-energy rovibrational dynamics of the $H_{5-n}D_n^+$ systems. The global minimum of the PESs has C_{2v} point-group symmetry. There are three low-lying stationary points with D_{2d}, C_{2v}, and D_{2h} symmetries. The first two are first-order saddle points and are closer than 100 cm^{-1} in energy to the global minimum, while the third one is a second-order saddle point with a relative energy less than 200 cm^{-1}. There is a third first-order saddle point, which also has C_{2v} point-group symmetry, but it is more than 1500 cm^{-1} higher in energy than the global minimum and it hinders the internal rotation (scrambling) of the H_3^+ unit.

Both the ABPDVR and the XBB PESs have been employed during the present study. The parameters of the XBB PES were taken from the iopenshell webpage,[46] which are slightly different from those presented in Ref. 20. Although the implementation of the XBB PES runs faster for a single point than that of the ABPDVR PES, convergence of the Lanczos algorithm is considerably quicker with the ABPDVR PES. This is part of the reason why the ABPDVR PES is applied in this study for the computation of selected vibrational eigenstates of all of the isotopologues and isotopomers. The XBB PES is used only for H_5^+ and D_5^+ to verify the results, to provide a comparison of the two surfaces, and to allow a comparison with previous studies, especially with DMC computations, which mostly applied the XBB PES.

When performing nuclear-motion computations with GENIUSH, it is important to choose an appropriate reference structure which facilitates the determination of an optimal DVR basis set. Take, as an example, NH_3, a non-rigid molecule with a large-amplitude motion due to the double-well nature of the PES. NH_3 has an equilibrium structure of C_{3v} point-group symmetry, while the transition state (TS) connecting the two equivalent minima of the double-well potential is planar with D_{3h} point-group symmetry. Both the C_{3v} minimum and the D_{3h} TS structures can be used as reference structures in nuclear motion computations,[43] resulting in the same energy levels when the computations are converged. While for the study of tunneling splittings the D_{3h} structure appears to be the preferred reference, when using smaller, "incomplete" basis sets the C_{3v} reference structure results in slightly better converged eigenstates.

In the case of H_5^+, although the global minimum has C_{2v} point-group symmetry, the zero-point averaged effective structure has D_{2d} point-group symmetry. Since the 1D potential along the z coordinate is asymmetric without the relaxation of the other coordinates (see Figure S1 in the supplementary material[47]), the relatively small number of basis functions applied may not give a proper, equal description of the two equivalent minima for the proton-hopping vibration. Freezing the inactive coordinates to the proton-hopping transition state structure D_{2d} instead of C_{2v} results in a 1D potential which is symmetric along the z coordinate and gives a more balanced description of the system around the two equivalent minima. Therefore, it seemed worth comparing the eigenvalues and eigenvectors computed with the two different reference structures (C_{2v} vs. D_{2d}), see below.

Use of the TS reference structure appears to yield a better description of the vibrational states of H_5^+ and its isotopomers, while the C_{2v} equilibrium structure seems to be better for the determination of the ZPVE. Therefore, computations were performed with both reference structures to determine the ground vibrational state, while the D_{2d} reference structure was used to determine the excited vibrational states.

The accurate geometry parameters of the C_{2v} and D_{2d} reference structures are given in Table I for the two PESs utilized in this study. Note that the D_{2d} structures employed are not exactly the D_{2d} stationary points of the PESs. Although the values of the θ_1, θ_2, x, y, and ϕ coordinates are the same, the values of R, z, r_1, and r_2 are the "averages" of the values at the two C_{2v} minima. The Cartesian coordinates and the corresponding energy values of the global minima of the two PES versions we utilized are very slightly different from the corresponding values originally reported in Refs. 20–22. Since these differences may cause small deviations especially notable in the computed ZPVEs, the exact values are given in the supplementary material.[47]

D. Basis sets

The basis functions corresponding to the different internal coordinates of H_5^+ are given in Table I. The ranges of the coordinates employed vary for the different coordinates (see also Table I). Potential-optimized DVR (PO-DVR)[48–50] functions were employed along all the coordinates except ϕ and z. Due to the use of PO-DVR basis functions, there can be significant differences between the allowed and the actual grid ranges utilized for the different isotopomers.

A direct-product basis set is employed in all nuclear-motion computations of this study. The size of the final basis set is one of the cost-determining factors during the computation of the required eigenvalues and eigenfunctions.

In reduced-dimensional computations the vibrational basis set was chosen to be as large as deemed necessary to compute energy levels converged to better than 0.1 cm^{-1}. As we are probing vibrational states which are relatively low in energy, basis functions for the two H–H stretch motions are somewhat less important and thus the number of corresponding basis functions is kept relatively small. In full-dimensional computations the vibrational basis set is as large as 2×10^8, requiring substantial computational resources to obtain the desired eigenvalues and eigenvectors: the largest standard computations yielding the results in the tables used a maximum of 450 GB of memory and about 11 000 h of CPU time on a single processor (note that the GENIUSH code is well parallelized), while the limited number of computations performed to verify the convergence used more than 1 TB of memory and 25 000 h of CPU time.

III. LARGE-AMPLITUDE MOTIONS (LAMS)

H_5^+ can be characterized by having several LAMs with low barriers. All of these motions play a crucial role in the understanding of the internal dynamics of the molecular ion. The first and most important LAM is the torsional motion (T) of the two formal H_2 units, which has an electronic barrier around 100 cm^{-1}.[21] H_5^+ is characterized by a symmetric and an antisymmetric torsional fundamental, ν_{TE} and ν_{TO}, respectively. As discussed previously,[8] this torsion plays a very important role in the understanding of the rotational-vibrational energy level structure of the molecule.[7,8,36] This motion provides facile exchange of the H and D atoms on the same side, left or right.

The second LAM is "proton hopping" (PH), the motion of the internal (middle) proton along the z axis (see Figure 1), while the molecule changes from one of the global minimum structure with C_{2v} point-group symmetry to the other. This motion clearly switches the left- and right-hand sides of the molecule. The electronic barrier associated with this motion is only around 50 cm^{-1} and has D_{2d} point-group symmetry.[21] Note, however, that the nuclear motion effectively eradicates the barrier.

The third LAM is the scrambling (SC) motion, i.e., the internal rotation of the formal H_3^+ unit. The C_{2v} point-group symmetry barrier to this motion is relatively large, about 1500 cm^{-1}.[21]

These three LAMs are responsible for the complete exchange of all the atoms of the molecular ion. The question whether one can scramble all the atoms of the ion becomes especially relevant upon deuteration, exchanging at least one H with D.

A fourth LAM also exists, which is the separation of the formal H_3^+ and H_2 units of the molecule, corresponding to the $H_5^+ \rightarrow H_3^+ + H_2$ dissociation (D) reaction. This motion has left and right symmetry. The first dissociation energy of the molecular ion, D_e, is about 2900 cm^{-1}, decreasing to about 2300 cm^{-1} when the zero-point vibrations are considered.

IV. ISOTOPOLOGUES AND ISOTOPOMERS OF H_5^+

Since all of the atoms are identical in the H_5^+ and D_5^+ molecular ions, they have only one isotopomer, $[H_2–H–H_2]^+$ and $[D_2–D–D_2]^+$, respectively, following the notation [left–middle–right]$^+$. When needed, the formal H_3^+ unit of the ion can be indicated in parentheses, as in $[(DH–H)–H_2]^+$.

Upon deuteration, five different positions are available for the first deuterium, suggesting five different isotopomers. However, due to the very small barriers hindering the torsional and proton-hopping motions (cf., Sec. III), the two atomic positions at the left and at the right, as well as the left and right sides become equivalent. Since the scrambling motion, which could exchange the inner and outer atoms of the formal H_3^+ unit of the cluster, has a relatively sizable barrier, this exchange does not seem to occur at low excitation energies. Due to these

TABLE II. Zero-point vibrational energies of the different deuterated H_5^+ isotopomers computed with GENIUSH. The results correspond to the basis set defined in Table I.[a]

		ABPDVR PES[21]					XBB PES[20]				
Isotopologue	Isotopomer	D_{2d}	C_{2v}	C'_{2v}	δ_1	δ_2	D_{2d}	C_{2v}	C'_{2v}	δ_1	δ_2
H_5^+	$[H_2–H–H_2]^+$	7242.0	7241.6		−0.45		7216.0	7213.1		−2.86	
H_4D^+	$[H_2–D–H_2]^+$	6895.8	6895.1		−0.74		6869.1	6866.0		−3.05	
	$[DH–H–H_2]^+$	6847.2	6846.0	6847.1	−1.19	−0.09	6821.3	6818.1	6819.5	−3.25	−1.83
$H_3D_2^+$	$[DH–D–H_2]^+$	6488.3	6487.1	6487.9	−1.23	−0.38	6461.6	6457.6	6460.0	−3.99	−1.63
	$[DH–H–DH]^+$	6452.2	6451.8		−0.33		6426.6	6424.5		−2.08	
	$[D_2–H–H_2]^+$	6403.6	6403.4	6403.6	−0.18	0.04	6378.2	6374.6	6377.0	−3.55	−1.14
$H_2D_3^+$	$[DH–D–DH]^+$	6086.2	6086.0		−0.22		6059.9	6057.7		−2.22	
	$[D_2–D–H_2]^+$	6029.6	6028.5	6029.2	−1.10	−0.41	6003.4	5998.6	6002.5	−4.75	−0.88
	$[D_2–H–DH]^+$	6008.0	6008.1	6008.1	0.03	0.05	5982.8	5980.5	5981.6	−2.29	−1.24
HD_4^+	$[D_2–D–DH]^+$	5631.0	5631.1	5631.6	0.05	0.61	5605.5	5602.7	5604.4	−2.82	−1.12
	$[D_2–H–D_2]^+$	5562.8	5562.8		−0.03		5537.9	5536.6		−1.32	
D_5^+	$[D_2–D–D_2]^+$	5179.5	5179.4		−0.10		5154.1	5152.7		−1.42	

[a]In the cases of less symmetric isotopomers, there are two possible choices of a C_{2v} reference structure, denoted without and with a prime (e.g., for $[DH–H–H_2]^+$, C_{2v} refers to $[DH–(H–H_2)]^+$, while C'_{2v} refers to $[(DH–H)–H_2]^+$, see the text for details). $\delta_1 := ZPVE(C_{2v}) - ZPVE(D_{2d})$, $\delta_2 := ZPVE(C'_{2v}) - ZPVE(D_{2d})$.

TABLE III. Zero-point vibrational energies of the different deuterated H_5^+ isotopomers; in case of GENIUSH, the results correspond to the basis set defined in Table I.

		ABPDVR PES[21]			XBB PES[20]			
Isotopologue	Isotopomer	GENIUSH	DMC[30]	MCTDH[28]	GENIUSH	DMC[a]	MCTDH[28]	DMC[23]
H_5^+	$[H_2–H–H_2]^+$	7242.0	7234.1	7237.5	7213.1	7205.2/7204.5	7202.6	7208
H_4D^+	$[H_2–D–H_2]^+$	6895.8	6887.9	6888.7	6866.0	6857.9/6857.5	6854.1	6860
	$[DH–H–H_2]^+$	6847.2	6840.2		6818.1	6812.0/6811.9	6811.4	6816
$H_3D_2^+$	$[DH–D–H_2]^+$	6488.3	6480.7		6457.6	6452.6/6452.1	6449.9	6457
	$[DH–H–DH]^+$	6452.2	6445.0		6424.5	6418.6/6418.9	6421.8	6420
	$[D_2–H–H_2]^+$	6403.6	6396.4		6374.6	6371.1/6371.8	6369.2	6374
$H_2D_3^+$	$[DH–D–DH]^+$	6086.2	6079.1		6057.7	6051.1/6052.6	6051.6	6055
	$[D_2–D–H_2]^+$	6029.6	6022.4		5998.6	5995.3/5996.5	5992.0	6000
	$[D_2–H–DH]^+$	6008.0	6001.1		5980.5	5976.3/5977.6	5979.0	5980
HD_4^+	$[D_2–D–DH]^+$	5631.0	5624.1		5602.7	5598.6/5600.6	5598.5	5603
	$[D_2–H–D_2]^+$	5562.8	5555.5	5562.0	5536.6	5533.0/5534.8	5535.6	5533
D_5^+	$[D_2–D–D_2]^+$	5179.5	5171.7	5177.9	5152.7	5149.0/5151.8	5151.0	5151

[a]The results left of the separator are those of Ref. 30, the results right of the separator are new results communicated to us by Anne McCoy, and were obtained using the same mass for D as employed in this study, $m_D = 2.014\,102$ u.

TABLE IV. Vibrational states of H_5^+ and D_5^+ corresponding to motions along the torsion (TE and TO, with E = even and O = odd, ϕ), the proton hopping (PH, z), and the H_2 dissociation (D, R) coordinates, obtained with two different PESs, ABPDVR,[21] and XBB.[20]

	H_5^+			D_5^+		
Label	ABPDVR	XBB	δ[a]	ABPDVR	XBB	δ[a]
ν_{TE}	90.0	87.3	2.7	35.3	33.2	2.1
ν_{TO}	135.8	138.7	−2.9	82.0	85.7	−3.8
ν_{PH}	352.3	353.9	−1.6	224.4	232.4	−7.9
$2\nu_{TE}$	445.6	444.0	1.6	224.6	224.3	0.2
$2\nu_{TO}$	446.3	446.8	−0.4	227.8	230.4	−2.6
$\nu_{PH}+\nu_{TE}$	446.9	446.8	0.1	262.1	269.1	−7.0
$\nu_{PH}+\nu_{TO}$	483.0	485.7	−2.8	301.8	310.9	−9.0
ν_D	653.4	636.9	16.5	461.4	454.9	6.5
$\nu_D+\nu_{TE}$[b]	750.0	731.4	18.6	495.4	489.9	5.5
$\nu_D+\nu_{TO}$	783.7	768.3	15.3	538.0	533.1	4.9
$\nu_{PH}+2\nu_{TE}$	797.7	797.2	0.5	447.0	454.0	−7.0
$\nu_{PH}+2\nu_{TO}$	798.3	798.8	−0.5	449.5	457.9	−8.4
$\nu_D+\nu_{PH}$	931.2	910.4	20.8	675.3	666.0	9.2
$3\nu_{TO}$	993.4	991.2	2.2	498.4	498.3	0.0
$3\nu_{TE}$[b]	993.4	991.1	2.3	503.1	501.3	1.8
$\nu_D+\nu_{PH}+\nu_{TE}$	1031.6	1008.3	23.3	713.1	704.4	8.7
$\nu_D+\nu_{PH}+\nu_{TO}$	1059.7	1039.9	19.8	749.5	742.0	7.5
$\nu_D+2\nu_{TO}$	1101.7	1083.4	18.3	686.3	679.9	6.3
$\nu_D+2\nu_{TE}$	1101.9	1082.8	19.1	684.0	676.4	7.6
$2\nu_D$	1153.5	1127.6	25.9	869.8	849.7	20.1
$2\nu_D+\nu_{TE}$	1253.2	1224.3	28.9	909.7	888.5	21.3
$2\nu_D+\nu_{TO}$	1281.7	1256.8	24.9		923.0	
$\nu_{PH}+3\nu_{TO}$	1344.8	1342.6	2.2	719.6	725.5	−5.9
$\nu_{PH}+3\nu_{TE}$	1344.8	1342.6	2.2	722.4	727.6	−5.2
$\nu_D+\nu_{PH}+2\nu_{TO}$	1380.3	1358.5	21.8	899.5	890.2	9.4
$\nu_D+\nu_{PH}+2\nu_{TE}$	1382.3	1360.6	21.8	897.6	887.2	10.4
$4\nu_{TE}$				878.7	877.9	0.8
$4\nu_{TO}$				878.7	877.9	0.8
$\nu_D+3\nu_{TE}$					950.2	

[a]δ = the difference between the results obtained with the ABPDVR and XBB PESs.
[b]In the case of D_5^+, the $\nu_D+\nu_{TE}$ and $3\nu_{TE}$ levels appear to be mixed when the ABPDVR PES is used.

characteristics of the BO-PES of H_5^+, from the five possible isotopomers of H_4D^+ only two will be different: $[H_2–D–H_2]^+$ and $[H_2–H–HD]^+$. Similarly, for the D_4H^+ isotopologue there are also only two different isotopomers: $[D_2–H–D_2]^+$ and $[D_2–D–HD]^+$. For the $H_3D_2^+$ isotopologue the situation is slightly more complex, three isotopomers seem to exist and the possible structures are $[DH–D–H_2]^+$, $[DH–H–DH]^+$, and $[D_2–H–H_2]^+$. Similarly, $[DH–D–DH]^+$, $[D_2–D–H_2]^+$, and $[D_2–H–DH]^+$ are the isotopomers of $H_2D_3^+$.

In conclusion, there are six different deuterated isotopologues of H_5^+ and these isotopologues define 12 different isotopomers, as supported by the results of the variational vibrational computations discussed in detail in Sec. V.

V. RESULTS AND DISCUSSION

The 60 vibrational energy levels computed for each of the 12 isotopomers, without detailed assignment, are reported in Tables S1 and S2 of the supplementary material.[47] For H_5^+ and D_5^+ both the XBB and ABPDVR PESs have been utilized, see Table S1.[47] For all the other deuterated isotopomers, the vibrational energy levels reported in Table S2[47] are based solely on the ABPDVR[21] PES. All these energies serve as benchmark results for future studies, their precision should be around 1–2 cm^{-1} for about the first 20 levels and increasingly lower above.

In our detailed discussion we focus first on ZPVEs of the isotopomers. The detailed first-principles results of the present study are given in Table II, while literature values are also reported in Table III. Then, we discuss the vibrations of H_5^+ and D_5^+, whereby some of the present results can be compared with literature values, see Tables IV to VI. Finally, results for the remaining isotopologues are presented, see Tables VII to XI, for which the present values serve as benchmark results, as the vibrational states of these isotopologues were not studied before. Discussion of the characteristics of the vibrational states is illuminated by a number of figures. In particular, two-dimensional (2D) wavefunction cuts are presented in Figures 2–7.

TABLE V. Vibrational states of H_5^+ and D_5^+, obtained with the ABPDVR[21] and XBB[20] PESs, corresponding to the four bending-type motions.

H_5^+				D_5^+			
Label	ABPDVR	XBB	δ[a]	Label	ABPDVR	XBB	δ[a]
$(\nu_{\theta_2}-\nu_y)+\nu_{TE}$	784.1	793.8	−9.7	$(\nu_{\theta_2}-\nu_y)+\nu_{TE}$	573.4	583.7	−10.3
$(\nu_{\theta_1}+\nu_x)$	785.1	794.9	−9.8	$(\nu_{\theta_1}+\nu_x)$	573.7	584.1	−10.3
$(\nu_{\theta_2}-\nu_y)$	862.5	866.6	−4.1	$(\nu_{\theta_2}-\nu_y)$	610.7	617.5	−6.8
$(\nu_{\theta_1}+\nu_x)+\nu_{TE}$	864.4	869.0	−4.6	$(\nu_{\theta_1}+\nu_x)+\nu_{TE}$	611.2	618.0	−6.8
$\nu_y+\nu_{PH}+\nu_{TE}$	963.9	968.5	−4.5	$(\nu_{\theta_1}+\nu_x)+2\nu_{TE}$	693.5	705.0	−11.6
$(\nu_{\theta_1}-\nu_x)-(\nu_{\theta_2}-\nu_y)+\nu_{PH}$	966.3	971.8	−5.5	$(\nu_{\theta_2}-\nu_y)+\nu_{TO}$	693.7	705.3	−11.7
$(\nu_{\theta_1}+\nu_x)+\nu_{D_{(-)}}+2\nu_{TE}$	1005.9	1011.9	−6.0	$(\nu_{\theta_2}-\nu_y)+\nu_{PH}+\nu_{TO}$	716.7	725.6	−8.9
$(\nu_{\theta_2}-\nu_y)+\nu_{TO}$	1006.0	1012.2	−6.2	$(\nu_{\theta_1}+\nu_x)+\nu_{PH}+2\nu_{TE}$	717.9	726.9	−9.0
$(\nu_{\theta_2}-\nu_y)+\nu_{PH}$	1010.5	995.7	14.8	$(\nu_{\theta_2}+\nu_y)+\nu_{PH}$	744.0	752.4	−8.4
$(\nu_{\theta_1}+\nu_x)+\nu_{PH}+\nu_{TO}$	1041.5	1034.6	7.0	$\nu_{\theta_1}+\nu_{PH}+\nu_{TE}$	746.3	754.2	−7.9
$\nu_{\theta_1}+\nu_{PH}+\nu_{TO}$	1064.0	1058.3	5.6	$(\nu_{\theta_1}+\nu_x)+\nu_{\theta_2}+2\nu_{TO}$	756.7		
$\nu_{\theta_2}+\nu_{PH}+2\nu_{TO}$	1069.6	1067.2	2.5	$(\nu_{\theta_1}+\nu_x)+\nu_{\theta_2}+2\nu_{TO}+\nu_{D_{(-)}}$		762.0	
$\nu_y+\nu_{TE}$	1088.0	1079.9	8.0	$(\nu_{\theta_1}-\nu_x)-(\nu_{\theta_2}-\nu_y)+\nu_{TO}$	758.3		
ν_x	1103.6	1104.3	−0.7	$(\nu_{\theta_1}-\nu_x)-(\nu_{\theta_2}-\nu_y)+\nu_{PH}+\nu_{TO}$		765.1	
$\nu_{\theta_1}+\nu_{D_{(-)}}+2\nu_{TO}$	1161.8			$\nu_y+\nu_{TE}$	799.7	810.1	−10.4
$(\nu_{\theta_1}+\nu_x)+\nu_{\theta_2}+2\nu_{TO}$		1154.6		ν_x	800.1	811.5	−11.4
$(\nu_{\theta_1}-\nu_x)+2\nu_{TE}$	1161.8			$\nu_y+\nu_{PH}+\nu_{TE}$	829.8	835.7	−6.0
$(\nu_{\theta_1}-\nu_x)+\nu_{TE}$		1152.8		$\nu_x+2\nu_{TE}$	833.8	839.8	−6.1
$\nu_y+\nu_{PH}+\nu_{TE}$	1163.2	1161.2	2.0	$(\nu_{\theta_1}+\nu_x)-(\nu_{\theta_2}+\nu_y)+2\nu_{TE}$	836.9	841.4	−4.5
$\nu_x+\nu_{D_{(-)}}$	1172.8	1169.7	3.0	$(\nu_{\theta_1}-\nu_x)+\nu_{TE}$	842.9	848.4	−5.5
$(\nu_{\theta_2}-\nu_y)+\nu_D+\nu_{TE}$	1208.2	1193.4	14.8	$\nu_{\theta_1}+\nu_{PH}+\nu_{TO}$	867.3	873.0	−5.7
$(\nu_{\theta_1}+\nu_x)+\nu_{D_{(+)}}$	1230.1	1216.3	13.8	$(\nu_{\theta_2}-\nu_y)+\nu_{PH}+\nu_{TE}$	869.0	875.9	−7.0
$\nu_{\theta_1}+\nu_{PH}+\nu_{TO}$	1235.2	1220.8	14.4	$(\nu_{\theta_1}+\nu_x)+\nu_{PH}+2\nu_{TO}$	874.7	883.5	−8.9
$\nu_y+\nu_D$	1242.5	1226.2	16.4	$\nu_{\theta_2}+\nu_D+2\nu_{TE}$	876.8		
$\nu_{\theta_2}+\nu_{PH}+2\nu_{TE}$	1261.0			$\nu_{\theta_2}+\nu_{PH}+2\nu_{TE}$		884.0	
$\nu_x+\nu_{PH}+\nu_{TE}$		1257.3		$(\nu_{\theta_2}-\nu_y)+\nu_D+\nu_{TE}$		913.0	
$\nu_{\theta_1}+\nu_{PH}+2\nu_{TO}$	1265.2	1264.2	1.1	$(\nu_{\theta_1}+\nu_x)+\nu_D$		917.0	
$(\nu_{\theta_2}-\nu_y)+\nu_{PH}+\nu_{TO}$	1266.7	1269.1	−2.4	$(\nu_{\theta_2}-\nu_y)+\nu_D$		929.9	
$\nu_x+\nu_{D_{(-)}}+\nu_{TE}$	1267.3			$(\nu_{\theta_1}+\nu_x)+\nu_D+\nu_{TE}$		937.3	
$\nu_x+\nu_{TE}$		1257.5		$\nu_{\theta_1}+\nu_y+2\nu_{TO}$		939.9	
				$\nu_{\theta_1}+\nu_D+3\nu_{TO}$		943.3	
				$\nu_{\theta_1}+2\nu_{TE}$		943.5	
				$\nu_{\theta_2}+\nu_x+\nu_{PH}+3\nu_{TE}$		949.5	

[a]δ = the difference between results obtained with the ABPDVR and XBB PESs.

TABLE VI. Vibrational energy levels of H_5^+ and D_5^+ obtained with GENIUSH for two different PESs, ABPDVR[21] and XBB,[20] as well as their computed and experimental counterparts from the literature.

		H_5^+								D_5^+					
		ABPDVR		XBB					Expt.	ABPDVR		XBB			Expt.
	Label	GENIUSH	Ref. 28	GENIUSH	Ref. 27	Ref. 28	Ref. 31	Ref. 29	Ref. 38	GENIUSH	Ref. 28	GENIUSH	Ref. 28	Ref. 29	Ref. 38
1	ν_{TE}	90.0	90.9	87.3	96.3	92.6	87.3			35.3	35.9	33.2	36.9		
2	ν_{TO}	135.8	136.2	138.7	135.7	133.3	138.7			82.0	82.3	85.7	81.5		
3	ν_{PH}	352.3	353.5	353.9	358.7	365.4	354.4	369	379	224.4	225.0	232.4	238.1	241	
4	$2\nu_{TE}$	445.6	449.4	444.0	452.9	447.1	444.0			224.6	227.0	224.3	225.0		
5	$2\nu_{TO}$	446.3	452.1	446.8	453.6	452.3	446.8			227.8	229.4	230.4	231.6		
6	$\nu_{PH}+\nu_{TE}$	446.9	449.7	446.8	464.4	462.8	447.3			262.1	263.5	269.1	278.2		
7	$\nu_{PH}+\nu_{TO}$	483.0	486.7	485.7	495.1	495.9	486.3			301.8	303.0	310.9	316.6		
8	ν_{D}	653.4	695.7	636.9	673.6	679.5	642.6	673		461.4	463.1	454.9	458.5	473	
9	$\nu_{D}+\nu_{TE}$	750.0	792.2	731.4	784.3	779.5	736.9			495.4	502.7	489.9	501.8		
10	$\nu_{D}+\nu_{TO}$	783.7	830.0	768.3	809.4	808.2	774.3			538.0	540.9	533.1	534.8		
11	$(\nu_{\theta_2}-\nu_y)+\nu_{TE}$	784.1	834.5	793.8	825.4	831.1				573.4	586.4	583.7	592.0		
12	$(\nu_{\theta_1}+\nu_x)$	785.1	835.9	794.9	846.0	834.7				573.7	586.1	584.1	592.2		
13	$\nu_{PH}+2\nu_{TE}$	797.7	814.7	797.2	822.0	819.8				447.0	452.3	454.0	463.9		
14	$\nu_{PH}+2\nu_{TO}$	798.3	818.3	798.8	825.3	826.9				449.5	452.7	457.9	472.2		
15	$(\nu_{\theta_2}-\nu_y)$	862.5	919.3	866.6	930.3	920.2				610.7	627.7	617.5	632.1		
16	$(\nu_{\theta_1}+\nu_x)+\nu_{TE}$	864.4	921.2	869.0	940.1	922.1				611.2	630.4	618.0			
17	$\nu_{D}+\nu_{PH}$	931.2	1072.8	910.4				983	940	675.3	687.6	666.0	511.0	713	679
18	$3\nu_{TO}$	993.4		991.2	1025.9	1019.1				498.4		498.3	511.0		
19	$3\nu_{TE}$	993.4		991.1	1017.2	1012.6				503.1		501.3	508.9		
20	$\nu_{D}+\nu_{PH}+\nu_{TE}$	1031.6		1008.3						713.1	692.7	704.4	632.2		
21	$\nu_{D}+\nu_{PH}+\nu_{TO}$	1059.7		1039.9						749.5	693.7	742.0	683.5		

A. Zero-point vibrational energies

The ZPVE values obtained with GENIUSH for the 12 isotopomers, using reference structures with both C_{2v} and D_{2d} point-group symmetry, are presented in Table II. The ZPVE energies determine the stability order of the distinct isotopomers of the isotopologues, the lower the ZPVE the more stable the molecular ion is. For this class of molecules the simple HO model fails to yield even qualitatively correct ZPVE estimates. The principal problem is that the HO model yields too many isotopomers, as it distinguishes between left and right; thus, it incorrectly yields three isotopomers for H_4D^+ and five for $H_3D_2^+$, for example. Nevertheless, even the HO model suggests that it is preferred to have H in the middle in the partially deuterated molecular ions.

Since the H–H stretchings have the highest contribution to the ZPVE, increasing the number of basis functions along these two coordinates may lead to an increase in the precision of the ZPVE determination. Doubling the number of basis functions along r_1 and r_2 for the ABPDVR[21] PES results in only a 0.3 cm^{-1} decrease in the ZPVE. Increasing the size of the basis along any of the other coordinates in a similar fashion has an even smaller effect, it changes the ZPVE only in the second decimal place. Thus, the ZPVE values computed appear to be rather precise.

Comparing the results of the computations using D_{2d} and C_{2v} reference structure reveals that the computation with the D_{2d} structure almost always results in larger values. The maximum difference is 1.2 cm^{-1} for the ABPDVR PES, while it is 4.8 cm^{-1} for the XBB[20] PES. This considerable difference can be due to the different description of the D_{2d} transition state region within the two surfaces (see Figure S2 in the supplementary materal[47]).

In the case of the C_{2v} reference structure, where the internal proton is not in the middle of the molecule, there is an issue with the choice of the C_{2v} reference structure for isotopomers where the diatomic units are different on the left and right sides. For symmetric isotopomers only one C_{2v} structure exists, but for the non-symmetric isotopologues formally there are two different ones. Take $[DH–H–H_2]^+$ as an example, where the two different C_{2v} structures are $[DH–(H–H_2)]^+$ and $[(DH–H)–H_2]^+$ (leading to the C_{2v} and C'_{2v} notation in Table II). Computations with these C_{2v} structures can result in slightly different ZPVE values, as the different reference structures determine slightly different grids used during the nuclear motion computations. In the four cases of the less symmetric isotopomers, one can compare the ZPVEs obtained with the different C_{2v} and the D_{2d} reference structures. First, for the ABPDVR PES, let us take a look at the isotopologues where one of the sides is H_2 and the other side is either HD or D_2. When the middle H or D atom is closer to the lighter H_2 side, the C_{2v} ZPVEs are smaller by up to 1.2 cm^{-1} than the D_{2d} one, while otherwise they are very close to the D_{2d} results: the differences are below 0.1 cm^{-1} with H in the middle and around 0.4 cm^{-1} with D in the middle. Second, consider the isotopologues where one side is D_2 and the other is HD. When the middle H or D atom is closer to the lighter HD side, the C_{2v} ZPVEs are slightly above the D_{2d} ones, while in the other case, when the middle H or D is closer to the D_2 side, the C_{2v} values can be

TABLE VII. Vibrational states of deuterated isotopologues of H_5^+ with homonuclear diatomics at the sides, corresponding to motions along the torsion (TE and TO, with E = even and O = odd, ϕ), the proton hopping (PH, z), and the $H_2(D_2)$ dissociation (D, R) modes and obtained with the ABPDVR PES.

Label	$[H_2–D–H_2]^+$	$[D_2–H–D_2]^+$	$[D_2–H–H_2]^+$	$[D_2–D–H_2]^+$
ν_{TE}	89.5	35.7	63.3	63.6
ν_{TO}	136.2	81.2	108.7	109.3
ν_{PH}	234.5	359.7	364.0	251.3
$2\nu_{TE}$	445.4	224.4	336.8	338.7
$2\nu_{TO}$	445.9	227.5	338.1	340.3
$\nu_{PH}+\nu_{TE}$	327.8	398.3	429.9	315.9
$\nu_{PH}+\nu_{TO}$	366.1	435.7	467.0	355.8
ν_{D}	523.0	575.2	627.5	507.9
$\nu_{D}+\nu_{TE}$	618.1	613.9	694.9	574.9
$\nu_{D}+\nu_{TO}$	653.1	651.7	729.9	611.1
$\nu_{PH}+2\nu_{TE}$	679.0	582.1	696.8	583.2
$\nu_{PH}+2\nu_{TO}$	679.4	584.4	698.1	584.5
$\nu_{D}+\nu_{PH}$	763.3	848.5	902.2	737.2
$3\nu_{TO}$	992.8	498.5	750.5	753.5
$3\nu_{TE}$	992.8	498.4	750.1	753.6
$\nu_{D}+\nu_{PH}+\nu_{TE}$	861.4	890.2	972.3	805.8
$\nu_{D}+\nu_{PH}+\nu_{TO}$	891.7	921.6	1002.4	838.0
$\nu_{D}+2\nu_{TO}$	968.1	800.4	964.9	844.2
$\nu_{D}+2\nu_{TE}$	969.2	798.3	963.9	843.3
$2\nu_{D}$	998.5	996.1	1090.1	954.0
$2\nu_{D}+\nu_{TE}$	1096.7	1035.7	1159.8	1023.1
$2\nu_{D}+\nu_{TO}$	1124.8			
$\nu_{PH}+3\nu_{TO}$		855.3	1105.7	990.7
$\nu_{PH}+3\nu_{TE}$		855.0	1105.7	990.7
$\nu_{D}+\nu_{PH}+2\nu_{TO}$		1071.5		
$\nu_{D}+\nu_{PH}+2\nu_{TE}$		1073.3		
$4\nu_{TE}$		878.9		
$4\nu_{TO}$		879.0		
$\nu_{D}+3\nu_{TO}$		1066.1		

considerably above the D_{2d} ones. For the XBB PES, the C_{2v} ZPVEs are always smaller than the D_{2d} ones.

In conclusion, for the ABPDVR PES we propose to accept the D_{2d} ZPVE values as more precise (see Table III for details), since they are very close to one set of C_{2v} values (the maximum difference is below 0.8 cm^{-1}). For the XBB PES, we propose to accept the first set of the C_{2v} ZPVE values as our final estimates (see Table III for details), since the D_{2d} values seem to have some systematic error. The arguments detailed above suggest that a conservative estimate of the precision of the present ZPVE estimates is about 5 cm^{-1}. Although DVR-based methods, such as GENIUSH, are not fully variational, it is tempting to conclude that the present values are upper estimates of the ZPVEs, and that the true, fully converged ZPVE values can be lower by as much as 5 cm^{-1} than the values chosen.

When the best ZPVE estimates are compared to the available DMC results (see Table III), it is seen that our computations give systematically larger ZPVE values, about 6-8 cm^{-1} for the ABPDVR PES, with a small spread, and 1-8 cm^{-1} for the XBB PES. The reason for the discrepancies larger than about 5 cm^{-1} remains basically unknown to us. One could argue that they are the result of slightly different parametrizations of the PESs used in this and the previous studies, resulting in slightly different energies at slightly different minima. One should also note that the DMC ZPVE values reported may also have an uncertainty of 3–5 cm^{-1}.

The variationally computed ZPVEs of the different isotopomers show that changing one of the H atoms of H_5^+ to D results in only two distinct molecules, i.e., isotopomers, one with the D in central position and the other with D on the side (Table III). For H_4D^+, the difference in the ZPVEs of the two isotopomers is 49 cm^{-1}. The analogous difference is larger, 68 cm^{-1}, for HD_4^+. Among the isotopologues with two isotopomers it is always the one with D in the middle which has the higher ZPVE. This can be easily understood by the large ZPVE contribution of the "side" H–H stretchings. As discussed above, substituting two Hs with Ds in the H_5^+ molecular ion results in three different structures. The ZPVE difference is 36 and 48 cm^{-1} from the "middle" for $H_3D_2^+$, while 57 and 21 cm^{-1} for $H_2D_3^+$.

In summary, for the mixed isotopologues the isotopomer with H in the middle is always more stable, i.e., has a lower ZPVE, than when H is at the side. This explains the stability order for the two forms of H_4D^+ and D_4H^+. For $H_2D_3^+$ and $H_3D_2^+$ there are three distinct isotopomers. Of course, the one with H in the middle is of lowest energy for $H_2D_3^+$. When there is a chance for forming homonuclear diatomics on the sides this isotopomer has the higher stability (lower ZPVE). Thus, two rules, "first, put H in the middle" and "second, form a

TABLE VIII. Vibrational states of deuterated isotopologues of H_5^+ with homonuclear diatomics at the sides corresponding to the four bending-type motions obtained with the ABPDVR[21] PES.

$[H_2–D–H_2]^+$		$[D_2–H–D_2]^+$		$[D_2–H–H_2]^+$		$[D_2–D–H_2]^+$	
Label	Value	Label	Value	Label	Value	Label	Value
$(\nu_{\theta_2}-\nu_y)+\nu_{TE}$	695.7	$(\nu_{\theta_2}-\nu_y)+\nu_{TE}$	620.0	$(\nu_{\theta_1}+\nu_x)$	636.7	$(\nu_{\theta_1}+\nu_x)$	569.0
$(\nu_{\theta_1}+\nu_x)$	696.7	$(\nu_{\theta_1}+\nu_x)$	620.1	$(\nu_{\theta_1}+\nu_x)+\nu_{TE}$	702.5	$(\nu_{\theta_1}+\nu_x)+\nu_{TE}$	627.2
$(\nu_{\theta_2}-\nu_y)$	737.7	$(\nu_{\theta_2}-\nu_y)$	668.4	$(\nu_{\theta_2}-\nu_y)+\nu_{TO}$	721.8	$(\nu_{\theta_2}-\nu_y)+\nu_{TO}$	648.2
$(\nu_{\theta_1}+\nu_x)+\nu_{TE}$	740.0	$(\nu_{\theta_1}+\nu_x)+\nu_{TE}$	668.6	$(\nu_{\theta_2}-\nu_y)$	827.1	$(\nu_{\theta_2}-\nu_y)$	670.7
$(\nu_{\theta_1}+\nu_x)+\nu_{PH}+\nu_{TO}$	816.2	$(\nu_{\theta_1}+\nu_x)+2\nu_{TE}$	746.8	$(\nu_{\theta_2}-\nu_y)+\nu_{TE}$	852.1	$(\nu_{\theta_2}-\nu_y)+\nu_{TE}$	751.7
$(\nu_{\theta_1}+\nu_x)+\nu_{PH}$	819.9	$(\nu_{\theta_2}-\nu_y)+\nu_{TO}$	746.9	ν_{θ_1}	863.4	$(\nu_{\theta_1}+\nu_x)+\nu_{PH}$	773.6
$(\nu_{\theta_2}-\nu_y)+\nu_{PH}$	832.5	$\nu_y+\nu_{TE}$	853.1	$\nu_{\theta_1}+2\nu_{TO}$	923.8	$\nu_{\theta_1}+\nu_{TO}$	790.3
$\nu_x+\nu_{PH}+\nu_{TO}$	848.5	ν_x	853.7	$\nu_{\theta_1}+\nu_{TO}$	927.2	$(\nu_{\theta_2}-\nu_y)+\nu_{PH}+\nu_{TE}$	818.1
$(\nu_{\theta_2}-\nu_y)+\nu_{TO}$	927.9	$(\nu_{\theta_1}+\nu_x)+(\nu_{\theta_2}-\nu_y)+\nu_{PH}+\nu_{TO}$	868.3	$\nu_{\theta_2}+\nu_{PH}+2\nu_{TE}$	947.5	$(\nu_{\theta_2}-\nu_y)+\nu_{D_{(-)}}$	818.6
$(\nu_{\theta_1}+\nu_x)+2\nu_{TO}$	930.1	$(\nu_{\theta_1}+\nu_x)+(\nu_{\theta_2}-\nu_y)+\nu_{PH}$	868.9	$(\nu_{\theta_2}-\nu_y)+\nu_{PH}+\nu_{TE}$	952.6	$(\nu_{\theta_1}+\nu_x)+\nu_{PH}+\nu_{TO}$	837.2
$(\nu_{\theta_1}+\nu_x)+\nu_{TO}$	938.1	ν_y	895.9	$\nu_y+\nu_{TO}$	990.9	$(\nu_{\theta_1}+\nu_x)+2\nu_{TO}$	852.6
$(\nu_{\theta_2}-\nu_y)+2\nu_{TO}$	949.2	$\nu_{\theta_1}+\nu_{TE}$	896.3	$\nu_y+\nu_{PH}$	1006.2	$(\nu_{\theta_1}+\nu_x)-(\nu_{\theta_2}+\nu_y)+\nu_{PH}+2\nu_{TO}$	868.5
$(\nu_{\theta_2}+\nu_y)+\nu_{TE}$	960.2	$(\nu_{\theta_2}-\nu_y)+3\nu_{TO}$	899.0	$\nu_y+\nu_{TE}$	1019.2	$\nu_{\theta_2}+\nu_{PH}+\nu_{TE}$	901.6
$(\nu_{\theta_1}+\nu_x)+2\nu_{TE}$	969.2	$(\nu_{\theta_1}+\nu_x)+2\nu_{TO}$	899.3	$(\nu_{\theta_1}+\nu_x)$	1027.1	ν_x	903.8
$(\nu_{\theta_2}-\nu_y)+\nu_D$	1014.3	$(\nu_{\theta_1}-\nu_x)$	948.0	$\nu_y+\nu_{TE}$	1032.3	$\nu_y+\nu_{TE}$	909.6
$(\nu_{\theta_1}+\nu_x)+\nu_{PH}+\nu_{TE}$	1028.3	$\nu_y+\nu_{TO}$	948.6	ν_{θ_2}	1064.7	$(\nu_{\theta_1}-\nu_x)+\nu_{TO}$	935.5
$\nu_x+\nu_{D_{(-)}}$	1037.5	$(\nu_{\theta_2}+\nu_y)$	1000.0	$(\nu_{\theta_1}-\nu_x)$	1095.7	$(\nu_{\theta_1}+\nu_x)+\nu_D$	961.8
$\nu_y+\nu_{D_{(+)}}+\nu_{TO}$	1038.5	$(\nu_{\theta_1}-\nu_x)+\nu_{PH}+\nu_{TO}$	1013.7	$\nu_{\theta_1}+\nu_D$	1104.4	$(\nu_{\theta_2}-\nu_y)+\nu_D$	962.2
$\nu_y+\nu_{D_{(-)}}+\nu_{TE}$	1047.0	$\nu_y+\nu_{PH}+\nu_{TE}$	1053.6	$\nu_x+\nu_{TE}$	1117.6	$2(\nu_{\theta_1}+\nu_x)$	1005.3
$\nu_x+\nu_{\theta_1}+\nu_{D_{(+)}}$	1060.9	$\nu_{\theta_1}+\nu_y+\nu_{PH}$	1061.0	$\nu_x+\nu_{TE}+\nu_{D_{(-)}}$	1155.1	$(\nu_{\theta_2}+\nu_y)$	1005.8
$\nu_x+\nu_{\theta_1}+\nu_{D_{(+)}}+\nu_{TO}$	1063.1	$\nu_{\theta_2}+\nu_D+\nu_{TO}$	1070.2	$(\nu_{\theta_2}-\nu_y)+\nu_{TO}+\nu_{D_{(-)}}$	1166.4	$\nu_x+\nu_{TE}+\nu_{D_{(-)}}$	1007.3
$\nu_y+\nu_{D_{(-)}}$	1065.5			$\nu_y+\nu_{TO}+\nu_D$	1178.6	$\nu_y+\nu_{TE}+\nu_{D_{(-)}}$	1008.0
$(\nu_{\theta_2}+\nu_y)+2\nu_{TE}$	1102.2			$\nu_{\theta_1}+\nu_{TE}+\nu_{PH}+\nu_{D_{(-)}}$	1181.7	$\nu_{\theta_1}+\nu_{PH}+2\nu_{TE}$	1012.7
$(\nu_{\theta_1}-\nu_x)+\nu_{TE}$	1102.3					$\nu_{\theta_1}+\nu_{TO}+\nu_{PH}+\nu_{D_{(-)}}$	1017.3
$(\nu_{\theta_2}+\nu_y)+\nu_{PH}+2\nu_{TO}$	1123.3					$\nu_y+\nu_{PH}+\nu_{TO}$	1032.4
$\nu_y+\nu_{PH}+\nu_{TO}$	1128.4					$\nu_x+2\nu_{TE}$	1032.9
$(\nu_{\theta_2}-\nu_y)+\nu_D+\nu_{PH}$	1184.1						

homonuclear diatomic at the side," explain the stability order for all cases investigated.

B. Vibrational states of H_5^+ and D_5^+

Characterization of the vibrational states of H_5^+ and D_5^+ is simplified by the fact that the H–H (and even the D–D) stretchings appear at an energy above the first dissociation asymptote. The two related motions do not enter the following discussion, as no states are computed for them. We arrange the motions characterizing the molecular ions into two groups. The first set, set I, of vibrational states to be discussed is characterized by motions along the torsion, the proton hopping, and the dissociation coordinates, i.e., ϕ, z, and R, respectively. In the second set, set II, we find the other states characterized principally by the four bending-type motions not mentioned, as well as their combination with the coordinates of the first set.

A specific characteristic of set I states is that they can be easily assigned by looking at wavefunction plots (see Figures 2–4). The standard rules of quantum chemistry are clearly applicable here: in the order of the energy levels first the fundamentals come and only then the appropriate overtones and combinations. For example, for $H_5^+(D_5^+)$ the ν_{PH} and ν_D fundamentals are at 352(224) and 653(461) cm^{-1}, respectively, while the $\nu_D + \nu_{PH}$ combination band is at 931(675) cm^{-1}, only −74(−10) cm^{-1} away from the simple sum of the fundamentals. It is an interesting exception from the standard rules that $2\nu_{PH}$ appears to be missing from the energy levels. Reduced-dimensional computations show that the $2\nu_{PH}$ overtone is completely missing, while its combination with ν_D comes only after $2\nu_D$, which is much higher in energy than expected.

It is also true for the set I states that most of them appear to be "pure," without extensive mixing. The only exceptions are the $\nu_D + \nu_{TE}$ and $3\nu_{TE}$ states of D_5^+ (and only with the ABPDVR PES); these states, in contrast to H_5^+, appear to be mixed with each other (see Figure S3 in the supplementary material[47] for details).

Upon perdeuteration, the mass scaling factor of $\sqrt{2}$ can be observed for most of the energy levels (see Table IV). The torsional levels, however, do not follow this rule and are scaled by about a factor of two.[7,8] This explains the absence of $4\nu_{TE}$ and $4\nu_{TO}$ of H_5^+ from Table IV, the pair should appear at about 1760 cm^{-1}, higher than the highest eigenvalue computed during this study.

TABLE IX. Vibrational states of deuterated isotopologues of H_5^+ with at least one heteronuclear diatomic at the sides, corresponding to motions along the torsion (TE and TO, with E = even and O = odd, ϕ), the proton hopping (PH, z), and the $H_2(D_2)$ dissociation (D, R) motions and obtained with the ABPDVR PES.

Label	$[DH–H–DH]^+$	$[DH–D–DH]^+$	$[DH–H–H_2]^+$	$[DH–D–H_2]^+$	$[D_2–H–DH]^+$	$[D_2–D–DH]^+$
ZPVE	6447.7	6081.7	6842.6	6483.3	6003.7	5626.9
ν_{TE}	61.8	60.9	76.0	75.6	48.8	48.3
ν_{TO}	107.0	107.1	121.5	121.8	94.0	94.5
ν_{PH}	353.4	226.1	355.4	237.4	358.0	229.8
$2\nu_{TE}$	330.4	328.5	388.7	388.2	277.7	277.2
$2\nu_{TO}$	332.1	330.2	389.9	389.3	279.8	279.6
$\nu_{PH}+\nu_{TE}$	418.9	290.0	435.3	315.7	409.9	280.3
$\nu_{PH}+\nu_{TO}$	455.2	328.7	471.7	354.6	446.7	319.7
ν_D	582.4	477.7	622.1	506.1	578.9	471.8
$\nu_D+\nu_{TE}$	649.3	543.1	703.4	586.4	632.8	523.6
$\nu_D+\nu_{TO}$	681.8[a]	578.5[a]	734.7[a]	622.0	676.7[a]	558.3[a]
	736.5[a]					
$\nu_{PH}+2\nu_{TE}$	682.3	552.7	742.4	622.6	633.3	503.8
$\nu_{PH}+2\nu_{TO}$	683.6	554.1	743.3	623.3	635.1	505.7
$\nu_D+\nu_{PH}$	841.3	691.0	882.9[a]	734.8	845.2	685.2
			949.5		926.4	
$3\nu_{TO}$	735.2	729.8	865.7	864.5	616.7	616.2
$3\nu_{TE}$	735.1	730.0	865.9	856.0[b]	616.5	616.0
				865.1		
$\nu_D+\nu_{PH}+\nu_{TE}$	911.2	757.3	966.6[a]	816.3	900.5	737.7
$\nu_D+\nu_{PH}+\nu_{TO}$	936.3[a]	799.9	1011.3[a]	851.7[a]	936.4	774.5[a]
	967.7[a]		1042.6			
$\nu_D+2\nu_{TO}$	921.3	805.2	1019.0	892.8	864.1	750.0
	930.4	824.9		900.6		
$\nu_D+2\nu_{TE}$	917.5	806.0	1014.9	893.6	859.0	747.3
$2\nu_D$	1020.5	900.1	1090.2[a]	953.7	1019.1[a]	888.1
			1183.9			
$2\nu_D+\nu_{TE}$	1101.6	966.9	1175.0	1031.1	1007.0[a]	942.4
				1042.3	1072.4	
$2\nu_D+\nu_{TO}$	1175.8		1233.1[a]	1068.4[a]	1108.4[a]	
$\nu_{PH}+3\nu_{TO}$	1078.5[a]	953.4	1217.2		971.5	839.4
	1087.1[a]					
$\nu_{PH}+3\nu_{TE}$	1084.7	952.3	1217.3		970.8	839.7
$\nu_D+\nu_{PH}+2\nu_{TO}$						966.2
$\nu_D+\nu_{PH}+2\nu_{TE}$					1126.0[a]	964.6
$4\nu_{TE}$					1085.7	
					1093.3[a]	
$4\nu_{TO}$					1079.0[c]	
					1088.5	

[a]The label is not exclusive, the state involves bending-type motions. See Tables X and XI for details.
[b]The lower eigenstate assigned as $3\nu_{TE}$ appears to be slightly perturbed.
[c]The label is not exclusive, the $4\nu_{TO}$ is mixed with $\nu_{D_{(-)}}$.

Comparison of the computed energy levels with the limited number of experimentally observed fundamentals, available for H_5^+ and D_5^+, shows significant disagreement (see Table VI). This suggests that the accuracy of the PESs of H_5^+ should be improved to obtain quantitative agreement between experiment and theory.

It is important to note that the two PESs employed yield rather similar vibrational energy levels, the two sets of levels agree with each other mostly within a few cm^{-1}. As the energy values presented in Table VI show, previous computations of vibrational states utilizing the two available PESs are in some disagreement. This is especially relevant for the published MCTDH energy levels. Thus, for an astructural molecule extreme care should be exercised when approximating the PES and doing the MCTDH computations afterwards. Finally, the close agreement between the limited number of energy levels computed by Song *et al.*[31] with those of the present study is encouraging and confirms the precision of the lowest energy levels of this study.

A significant difference between the energy values obtained with the two PESs is that the torsional splittings are significantly larger for the XBB PES. For H_5^+, the XBB PES yields 51.5, 2.8, and 0.1 cm^{-1} splittings for the first three torsional modes, while they are 45.8, 0.8, and 0.1 cm^{-1} for the ABPDVR PES. For D_5^+, the torsional splittings are larger, especially for $2\nu_T$. For $n\nu_T$, $n = 1,2,3,4$, they are 52.5, 6.1, 3.0, and 0.0 cm^{-1} for the XBB PES, and 46.7, 3.2, 4.7, and 0.0 cm^{-1} for the ABPDVR PES. It is strange to see within the

TABLE X. Vibrational states of four deuterated isotopologues of H_5^+ with at least one heteronuclear diatomic at the sides, corresponding to the four bending-type motions and obtained with the ABPDVR[21] PES.

$[DH–H–H_2]^+$		$[DH–D–H_2]^+$		$[D_2–H–DH]^+$		$[D_2–D–DH]^+$	
Label	Value	Label	Value	Label	Value	Label	Value
$(\nu_{\theta_1}+\nu_x)+\nu_D$	725.3	$(\nu_{\theta_1}+\nu_x)+\nu_{PH}$	628.8	$(\nu_{\theta_1}+\nu_x)+\nu_{D_{(+)}}+3\nu_{TO}$	629.7	$\nu_D+\nu_{TO}+(\nu_{\theta_1}+\nu_x)$	558.3[a]
$\nu_D+\nu_{TO}+(\nu_{\theta_2}-\nu_y)$	734.7[a]	$(\nu_{\theta_2}-\nu_y)+\nu_{TO}$	684.3	$\nu_D+\nu_{TO}+(\nu_{\theta_1}+\nu_x)$	676.7[a]	$(\nu_{\theta_1}+\nu_x)+\nu_{TO}$	579.7
$(\nu_{\theta_2}-\nu_y)+\nu_{TO}$	778.5	$(\nu_{\theta_1}+\nu_x)+\nu_{TE}$	685.2	$(\nu_{\theta_1}+\nu_x)+\nu_{TE}$	687.4	$(\nu_{\theta_1}+\nu_x)+\nu_{TE}$	622.5
$(\nu_{\theta_1}+\nu_x)+\nu_{TE}+\nu_D$	800.4	$(\nu_{\theta_2}-\nu_y)$	708.6	$(\nu_{\theta_2}-\nu_y)+\nu_D+\nu_{TO}$	693.0	$(\nu_{\theta_2}-\nu_y)+\nu_{TO}$	622.5
$(\nu_{\theta_2}-\nu_y)$	847.9	$(\nu_{\theta_2}-\nu_y)+\nu_{PH}+\nu_{TE}$	795.5	$(\nu_{\theta_2}-\nu_y)+\nu_D+\nu_{TE}$	773.1	$(\nu_{\theta_2}-\nu_y)$	662.9
$\nu_D+\nu_{PH}+\nu_{\theta_1}$	882.9[a]	$(\nu_{\theta_1}+\nu_x)+\nu_{PH}$	810.9	$(\nu_{\theta_2}-\nu_y)+\nu_{TE}$	798.2	$(\nu_{\theta_2}-\nu_y)+\nu_{TE}$	724.2
$(\nu_{\theta_2}-\nu_y)+\nu_{TE}$	914.7	$(\nu_{\theta_2}-\nu_y)+\nu_{PH}$	818.4	$(\nu_{\theta_1}+\nu_x)+2\nu_{TE}$	845.3	$(\nu_{\theta_1}+\nu_x)+\nu_{PH}+\nu_{TO}$	727.8
$\nu_D+\nu_{PH}+\nu_{TE}+\nu_{\theta_1}$	966.6[a]	$(\nu_{\theta_2}-\nu_y)+\nu_{PH}+\nu_{TO}$	838.5	$\nu_{\theta_1}+\nu_{TO}$	854.6	$(\nu_{\theta_2}-\nu_y)+\nu_{PH}+\nu_{TE}$	768.2
$\nu_{\theta_1}+\nu_D+2\nu_{TE}$	967.8	$\nu_D+\nu_{PH}+\nu_{TO}+\nu_{\theta_2}-\nu_y$	851.7[a]	$\nu_{\theta_1}+\nu_{TE}$	907.3	$\nu_y+\nu_{PH}+\nu_{TE}$	768.6
$\nu_{\theta_1}+\nu_{\theta_2}+\nu_{PH}+\nu_{TE}$	970.2	$\nu_{\theta_1}+3\nu_{TE}$	855.0	$\nu_{\theta_1}+\nu_y$	917.2	$\nu_D+\nu_{PH}+\nu_{TO}+(\nu_{\theta_1}+\nu_x)$	774.5[a]
$(\nu_{\theta_2}-\nu_y)+\nu_{PH}+2\nu_{TO}$	983.7	$(\nu_{\theta_1}+\nu_x)+\nu_{PH}+\nu_{TE}$	860.1	$(\nu_{\theta_1}+\nu_x)+2\nu_{TO}$	961.7	$(\nu_{\theta_1}+\nu_x)+\nu_{PH}+\nu_{TO}$	777.5
$\nu_D+\nu_{PH}+\nu_{TO}+\nu_y$	1011.3[a]	$(\nu_{\theta_2}-\nu_y)+2\nu_{TE}$	914.2	$(\nu_{\theta_2}-\nu_y)+\nu_{D_{(-)}}+\nu_{TO}$	971.6	$(\nu_{\theta_1}+\nu_x)+2\nu_{TO}$	781.7
$\nu_{\theta_1}+\nu_D+\nu_{PH}+\nu_{TE}$	1014.2	$(\nu_{\theta_2}+\nu_y)+\nu_{TE}$	924.3	$\nu_y+2\nu_{D_{(-)}}+\nu_{TE}$	977.4	$(\nu_{\theta_1}+\nu_x)+(\nu_{\theta_2}-\nu_y)+\nu_{PH}+2\nu_{TE}$	791.3
$(\nu_{\theta_2}+\nu_y)+\nu_{PH}+2\nu_{TE}$	1046.1	$(\nu_{\theta_1}-\nu_x)+2\nu_{TE}$	932.9	$(\nu_{\theta_2}-\nu_y)+\nu_D+\nu_{PH}+\nu_{TE}$	983.6	$\nu_{\theta_2}+\nu_{PH}+2\nu_{TE}$	813.7
$\nu_y+\nu_{TO}$	1053.8	$\nu_{\theta_1}+\nu_{D_{(+)}}+\nu_{PH}\nu_{TO}$	971.2	$2\nu_D+\nu_y+\nu_{TE}$	1007.0[a]	$\nu_x+2\nu_{TO}$	847.6
ν_x	1080.2	$\nu_{\theta_1}+(\nu_{\theta_2}-\nu_y)+\nu_{PH}+\nu_{TO}$	980.1	$\nu_{\theta_2}+2\nu_{D_{(-)}}+\nu_{TE}$	1009.2	$(\nu_{\theta_2}+\nu_y)+\nu_{TE}$	848.9
$2\nu_D+(\nu_{\theta_1}+\nu_x)$	1090.2[a]	$(\nu_{\theta_2}-\nu_y)+\nu_D$	988.7	$2\nu_D+(\nu_{\theta_2}-\nu_y)$	1019.1[a]	$\nu_{\theta_2}+\nu_{PH}+\nu_{TE}$	853.9
$\nu_{\theta_1}+\nu_y+\nu_{PH}+\nu_{TO}$	1098.5	$\nu_x+2\nu_D$	1003.9	$(\nu_{\theta_1}-\nu_x)+\nu_{TO}$	1039.3	$(\nu_{\theta_1}-\nu_x)+\nu_{TO}$	877.7
$(\nu_{\theta_1}+\nu_x)+\nu_{D_{(-)}}+\nu_{TE}$	1122.3	$\nu_y+\nu_D+\nu_{TE}$	1023.5	$(\nu_{\theta_1}-\nu_x)+\nu_{\theta_2}+\nu_{PH}+3\nu_{TO}$	1069.5	$\nu_{\theta_2}+2\nu_{D_{(-)}}+2\nu_{TE}$	902.9
$(\nu_{\theta_1}+\nu_x)+\nu_{\theta_2}+\nu_D+2\nu_{TE}$	1126.9	$(\nu_{\theta_1}-\nu_x)+\nu_{PH}+2\nu_{TE}$	1031.8	$(\nu_{\theta_1}+\nu_x)+\nu_{D_{(-)}}+\nu_{TO}$	1072.8	$(\nu_{\theta_1}+\nu_x)+\nu_{D_{(-)}}$	913.1
$(\nu_{\theta_1}+\nu_x)$	1142.2	$(\nu_{\theta_2}-\nu_y)+\nu_{PH}+2\nu_{TO}$	1042.9	$4\nu_{TE}+\nu_{PH}+(\nu_{\theta_1}+\nu_x)$	1093.3[a]	$(\nu_{\theta_1}-\nu_x)+\nu_{PH}+\nu_{TE}$	928.2
$(\nu_{\theta_2}-\nu_y)+\nu_{D_{(-)}}+\nu_{TE}$	1185.0	$(\nu_{\theta_2}+\nu_y)$	1046.5	$2\nu_D+\nu_{TO}+(\nu_{\theta_1}+\nu_x)$	1108.4[a]	$(\nu_{\theta_1}-\nu_x)+\nu_{PH}+2\nu_{TO}$	935.3
$(\nu_{\theta_1}+\nu_x)+\nu_{\theta_2}+\nu_y+\nu_{PH}+\nu_{TE}$	1198.5	$\nu_x+2\nu_D+\nu_{TE}$	1058.7	$\nu_D+\nu_{PH}+2\nu_{TE}+(\nu_{\theta_1}+\nu_x)$	1126.0[a]	$\nu_{\theta_2}+\nu_{PH}+\nu_{D_{(-)}}+2\nu_{TO}$	938.8
$\nu_y+\nu_{D_{(-)}}$	1203.5	$\nu_{\theta_1}+\nu_{D_{(-)}}+2\nu_{D_{(+)}}$	1064.0			$(\nu_{\theta_2}-\nu_y)+\nu_{D_{(-)}}+\nu_{TO}$	942.2
$(\nu_{\theta_2}-\nu_y)+\nu_{D_{(-)}}+\nu_{TO}$	1209.8	$2\nu_D+\nu_{TO}+\nu_y$	1068.4[a]			$(\nu_{\theta_1}+\nu_x)+\nu_{\theta_2}+\nu_D$	948.3
$(\nu_{\theta_1}-\nu_x)+\nu_{PH}+2\nu_{TE}$	1214.9	$(\nu_{\theta_1}-\nu_x)-(\nu_{\theta_2}-\nu_y)+\nu_{D_{(+)}}+\nu_{TO}$	1081.7			$\nu_y+\nu_D+\nu_{TE}$	971.6
$(\nu_{\theta_2}-\nu_y)+\nu_{D_{(+)}}+2\nu_{TE}$	1231.4	$(\nu_{\theta_1}+\nu_x)$	1088.8				
$2\nu_{D_{(-)}}+\nu_{TO}+(\nu_{\theta_1}-\nu_x)-(\nu_{\theta_2}+\nu_y)$	1233.1[a]						

[a]The not exclusive labels of Table IX are given here exclusively.

observed pattern that the splitting of $3\nu_T$ is larger than that of $2\nu_T$ for the ABPDVR PES. This is due to the above-mentioned mixing concerning the formally $n\nu_T$ series of states. The fast disappearance of the torsional splittings is also observable in the 1D torsion-only model, where the splittings are slightly smaller, starting from around 40 cm^{-1}, and become close to 0.0 cm^{-1} at $3\nu_T$ and $4\nu_T$ for H_5^+ and D_5^+, respectively. The splittings generally decrease when the torsional motion mixes with the other motions. The more extensive the mixing is, the larger is the decrease in the splittings. For H_5^+ and for the ABPDVR PES, for example, the splitting is 36.1, 33.7, and 28.1 cm^{-1} for the combination of ν_T with ν_{PH}, ν_D, and ν_{PH} + ν_D, respectively.

The vibrational energy levels of H_5^+ are smaller in general for the XBB PES than for the ABPDVR PES. One exception is the ν_{PH} state, which appears at a somewhat smaller energy for the ABPDVR PES. Eigenvalues with odd torsional excitation also give negative differences in Table IV, which lists differences, δ, between the energy levels obtained with the ABPDVR and the XBB PESs. This is due to the larger torsional splitting in the case of the XBB PES. For D_5^+, where the differences are larger between the vibrational levels corresponding to the two PESs, these effects are larger and there are almost twice as many negative δ values. The more substantial differences concern vibrational levels where the contribution of the dissociative motion, along R, is significant. For $H_5^+(D_5^+)$, for example, the differences in ν_D and $2\nu_D$ are 17(7) and 26(20) cm^{-1}, respectively. Interestingly, the differences are basically maintained for the combination bands, note the almost constant 19 cm^{-1} difference for the VBOs described as $\nu_D + \nu_{TE}$, $\nu_D + \nu_{TO}$, $\nu_D + \nu_{PH}$, $\nu_D + 2\nu_{TE}$, and $\nu_D + 2\nu_{TO}$, implicitly supporting the labels provided. A large part of the difference of 29 cm^{-1} between the ZPVEs provided by the two PESs is also seemingly due to the different description of this dissociative motion.

Although the 1D cuts of the two PESs along the dissociative coordinate look qualitatively the same (see the

TABLE XI. Vibrational states of two deuterated isotopologues of H_5^+ with heteronuclear diatomics at both sides, corresponding to the four bending-type motions and obtained with the ABPDVR[21] PES.

$[DH–H–DH]^+$		$[DH–D–DH]^+$	
Label	Value	Label	Value
$\nu_D+\nu_{TO}+(\nu_{\theta_1}+\nu_x)-(\nu_{\theta_2}-\nu_y)$	681.8[a]	$\nu_D+\nu_{TO}+(\nu_{\theta_1}+\nu_x)+(\nu_{\theta_2}-\nu_y)$	578.5[a]
$(\nu_{\theta_1}+\nu_x)+(\nu_{\theta_2}-\nu_y)+\nu_{PH}+\nu_{TE}$	715.1	$(\nu_{\theta_1}+\nu_x)-(\nu_{\theta_2}-\nu_y)+\nu_{TO}$	635.0
$\nu_D+\nu_{TO}+(\nu_{\theta_1}+\nu_x)-(\nu_{\theta_2}-\nu_y)$	736.5[a]	$(\nu_{\theta_1}+\nu_x)+(\nu_{\theta_2}-\nu_y)+\nu_D+\nu_{PH}+\nu_{TE}$	639.7
$(\nu_{\theta_1}+\nu_x)+(\nu_{\theta_2}-\nu_y)+\nu_{PH}+\nu_{TO}$	783.8	$(\nu_{\theta_1}+\nu_x)-(\nu_{\theta_2}-\nu_y)+\nu_{TE}$	680.1
$(\nu_{\theta_1}+\nu_x)+(\nu_{\theta_2}-\nu_y)+\nu_D+\nu_{TE}$	793.9	$(\nu_{\theta_1}+\nu_x)+(\nu_{\theta_2}-\nu_y)+\nu_D+\nu_{PH}+\nu_{TO}$	683.7
$(\nu_{\theta_1}+\nu_x)+(\nu_{\theta_2}-\nu_y)+\nu_D+\nu_{TO}$	876.4	$(\nu_{\theta_1}+\nu_x)+(\nu_{\theta_2}-\nu_y)+\nu_{D_{(-)}}+\nu_{PH}+\nu_{TO}$	757.7
$(\nu_{\theta_1}+\nu_x)+(\nu_{\theta_2}-\nu_y)+\nu_{PH}+\nu_{TO}$	882.3	$(\nu_{\theta_2}-\nu_y)+\nu_{PH}+\nu_{TO}$	763.3
$\nu_D+\nu_{PH}+\nu_{TO}+\nu_{\theta_1}+\nu_{\theta_2}$	936.3[a]	$\nu_x-(\nu_{\theta_2}-\nu_y)+\nu_{PH}+2\nu_{TE}$	794.6
$\nu_D+\nu_{PH}+\nu_{TO}+\nu_{\theta_1}+\nu_{\theta_2}$	967.7[a]	$\nu_x+\nu_{PH}+\nu_{TE}$	809.7
$\nu_{\theta_1}+\nu_D+\nu_{TE}$	982.2	$(\nu_{\theta_1}+\nu_x)+(\nu_{\theta_2}-\nu_y)+2\nu_{TE}$	827.7
$(\nu_{\theta_1}+\nu_x)-(\nu_{\theta_2}+\nu_y)+\nu_{PH}+\nu_{D_{(+)}}+2\nu_{TE}$	993.1	$(\nu_{\theta_1}+\nu_x)-(\nu_{\theta_2}-\nu_y)+\nu_D+\nu_{TO}$	846.0
$(\nu_{\theta_1}+\nu_x)+\nu_y+\nu_D+\nu_{PH}+\nu_{TO}$	1000.8	$\nu_{\theta_2}+\nu_{D_{(-)}}+\nu_{PH}+2\nu_{TE}$	853.0
$(\nu_{\theta_1}+\nu_x)+\nu_{\theta_2}+\nu_D+\nu_{PH}+\nu_{TE}$	1016.1	$(\nu_{\theta_1}-\nu_x)-(\nu_{\theta_2}+\nu_y)+\nu_{TE}$	877.8
$(\nu_{\theta_2}-\nu_y)+2\nu_D$	1036.4	$(\nu_{\theta_1}-\nu_x)+\nu_{PH}+2\nu_{TO}$	887.1
$(\nu_{\theta_1}+\nu_x)+(\nu_{\theta_2}-\nu_y)+\nu_{PH}+\nu_{TO}$	1041.7	$(\nu_{\theta_1}-\nu_x)-\nu_{\theta_2}+2\nu_{TO}$	929.0
$(\nu_{\theta_1}+\nu_x)-(\nu_{\theta_2}-\nu_y)+2\nu_{TO}$	1073.7	$\nu_{\theta_1}+\nu_{PH}$	931.6
$(\nu_{\theta_1}+\nu_x)+\nu_{\theta_2}+\nu_y+2\nu_{D_{(-)}}+2\nu_{TE}$	1076.3	$\nu_{\theta_2}+\nu_x+\nu_{D_{(+)}}+\nu_{TO}$	933.6
$\nu_{PH}+3\nu_{TO}+(\nu_{\theta_1}+\nu_x)+(\nu_{\theta_2}-\nu_y)$	1078.5[a]	$\nu_x+\nu_{D_{(-)}}+2\nu_{TO}$	937.0
$\nu_{PH}+3\nu_{TO}+(\nu_{\theta_1}+\nu_x)+(\nu_{\theta_2}-\nu_y)$	1087.1[a]	$(\nu_{\theta_2}-\nu_y)+\nu_{D_{(-)}}+\nu_{TE}$	972.3
$(\nu_{\theta_1}-\nu_x)+\nu_{D_{(-)}}+\nu_{TE}$	1092.1	$(\nu_{\theta_1}-\nu_x)-\nu_y+2\nu_D+\nu_{TE}$	973.2
$(\nu_{\theta_2}+\nu_y)+\nu_{D_{(-)}}+\nu_{TO}$	1126.1	$(\nu_{\theta_1}+\nu_x)+\nu_{D_{(+)}}$	979.2
$\nu_{\theta_2}+\nu_{PH}+\nu_{TO}$	1133.1	$\nu_{\theta_1}+\nu_{\theta_2}+2\nu_{TE}$	979.7
$\nu_{\theta_1}+\nu_{\theta_2}+2\nu_{D_{(+)}}+3\nu_{TE}$	1133.2	$(\nu_{\theta_1}-\nu_x)-\nu_{\theta_2}+\nu_{TO}$	999.0
$(\nu_{\theta_1}+\nu_x)-\nu_y+\nu_{PH}+\nu_{TE}$	1140.2	$\nu_y+2\nu_{D_{(-)}}+\nu_{D_{(+)}}$	1004.3
$(\nu_{\theta_1}+\nu_x)+\nu_{D_{(-)}}+\nu_{TE}$	1152.2	$(\nu_{\theta_1}+\nu_x)+\nu_{PH}+2\nu_{TO}$	1008.3
$(\nu_{\theta_2}+\nu_y)+\nu_{D_{(+)}}+2\nu_{TO}$	1155.4	$\nu_x+2\nu_{D_{(-)}}+\nu_{D_{(+)}}+\nu_{TO}$	1015.3
$\nu_y+\nu_D+\nu_{PH}+2\nu_{TE}$	1184.9		

[a]The not exclusive labels of Table IX are given here exclusively.

insets of Figure 8 for the R dependence) and show only slight deviations, especially at short and longer R values, there are essential differences between the two PESs. These can clearly be seen in Figure 8. These differences are relatively minor (ca. 100 cm^{-1}) around the position of the C_{2v} minimum (3.5–5.0 bohrs), but they increase to 2000 cm^{-1} for very small distances. Figure 8 also shows that the sign of the difference changes repeatedly along the R coordinate. These differences of the PESs cause the relatively large differences in the vibrational energy levels corresponding to the R coordinate and its combination modes (see Table IV).

The energy values of the set I vibrational states seem to be well converged. Increasing the size of the basis along the R, ϕ, and z coordinates using the same coordinate intervals, resulting in a Hamiltonian matrix of size 450M, yields changes of less than 0.1 cm^{-1} for the first 25 energy levels, which increases only to about 0.5 cm^{-1} for the second 25 levels. This implies that the motions along the R, ϕ, and z coordinates, corresponding to the ν_D, ν_T, and ν_{PH} fundamentals, are particularly well described. We also observed that the different reference structures during the GENIUSH computations do not influence the values of the set I vibrational energy levels and the shape of the wavefunctions (not shown).

The set II vibrational eigenstates correspond to motions along the θ_1, θ_2, x, and y coordinates, as well as to their combinations with ϕ, z, and R. In these cases characterization of the wavefunctions is much more problematic.

First, our choice of internal coordinates (see Figure 1) does not seem to correspond closely to the vibrational motions characteristic of the set II states. More appropriate coordinates, which are mostly used during the assignation (see the appropriate tables), would be the combination of θ_1 with x and θ_2 with y, resulting in the "$\theta_1 \pm x$" and "$\theta_2 \pm y$" descriptors. The "$\theta_1 + x$" and "$\theta_2 - y$" eigenstates can be characterized as symmetric, bending-type motions of the outer H_2 unit and the internal proton. These linear combinations, rather than the antisymmetric "$\theta_1 - x$" and "$\theta_2 + y$" ones, characterize the great majority of the bending vibrational states.

Second, in some cases the combination of the bending vibration with the other motions, especially ϕ, comes before the corresponding "pure" vibrational state (see Table V). This is the case for the first four bending states of H_5^+ and D_5^+, $(\nu_{\theta_2}-\nu_y)+\nu_{TE}$, $(\nu_{\theta_1}+\nu_x)$, $(\nu_{\theta_2}-\nu_y)$, and $(\nu_{\theta_1}+\nu_x)+\nu_{TE}$ (see Figure 5 for more details), and appears also at higher energies when these motions combine with R (for D_5^+ with the XBB PES, see Table V). These four levels are pairwise quasi-degenerate, $(\nu_{\theta_2}-\nu_y)+\nu_{TE}$ is paired with $(\nu_{\theta_1}+\nu_x)$ at 784(573) cm^{-1}, and $(\nu_{\theta_2}-\nu_y)$ is paired with $(\nu_{\theta_1}+\nu_x)+\nu_{TE}$ at 863(611) cm^{-1} for H_5^+ (D_5^+). This ordering

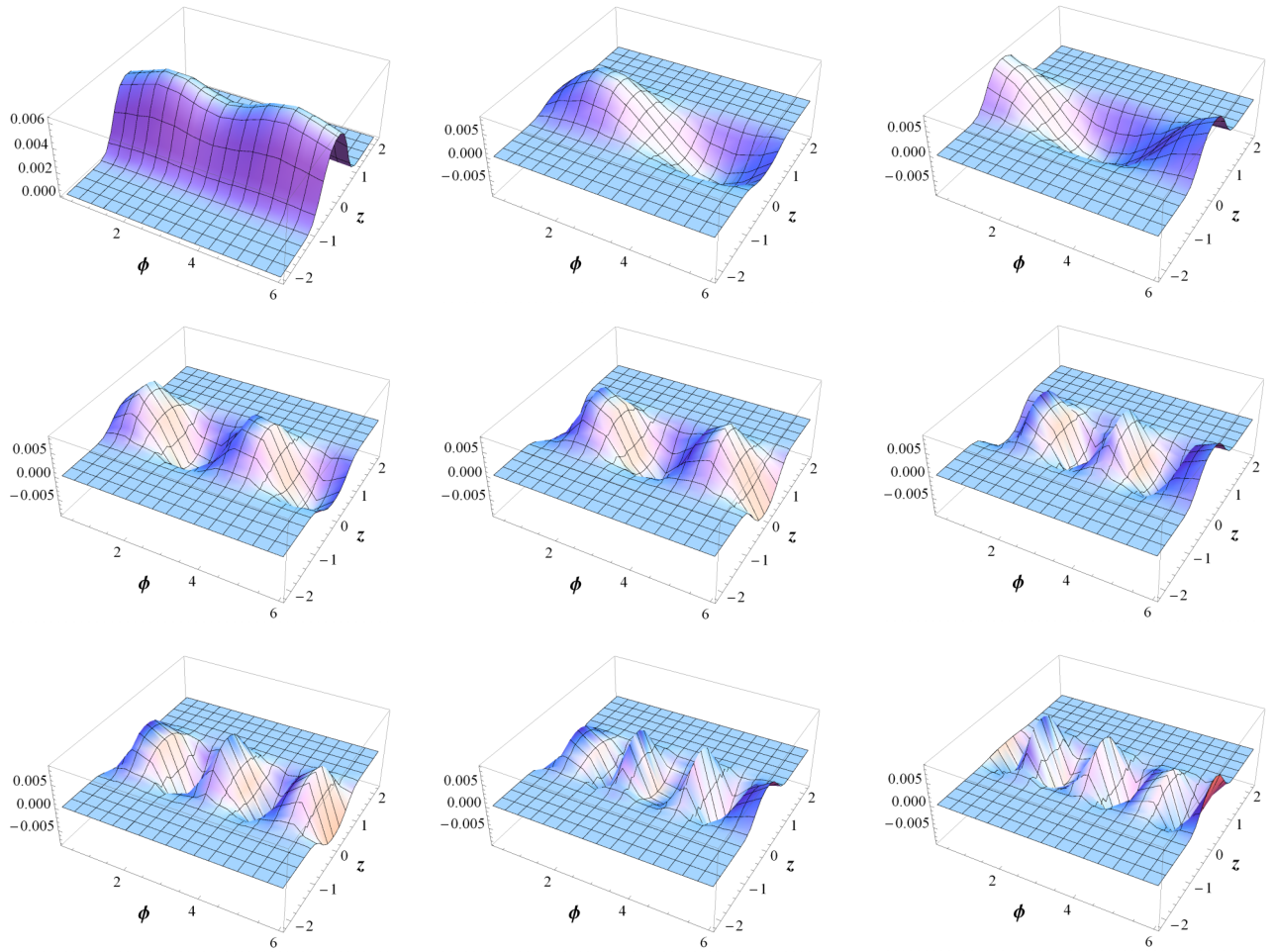

FIG. 2. 2D (ϕ, z) cuts of the 9D vibrational wavefunctions of the computed torsional eigenstates of H_5^+ (the figures are qualitatively the same for D_5^+); first row: (ν_{ZP}, ν_{TE}, ν_{TO}), second row: ($2\nu_{TE}, 2\nu_{TO}, 3\nu_{TE}$), and third row: ($3\nu_{TO}, 4\nu_{TE}, 4\nu_{TO}$).

FIG. 3. 2D (R, z) cuts of the 9D vibrational wavefunctions of the computed "proton-hopping" and dissociative eigenstates of H_5^+ (and D_5^+) with their overtones and combination bands; first row: (ν_{ZP}, ν_{PH}, ν_D), second row: ($\nu_{PH}+\nu_D, 2\nu_D$).

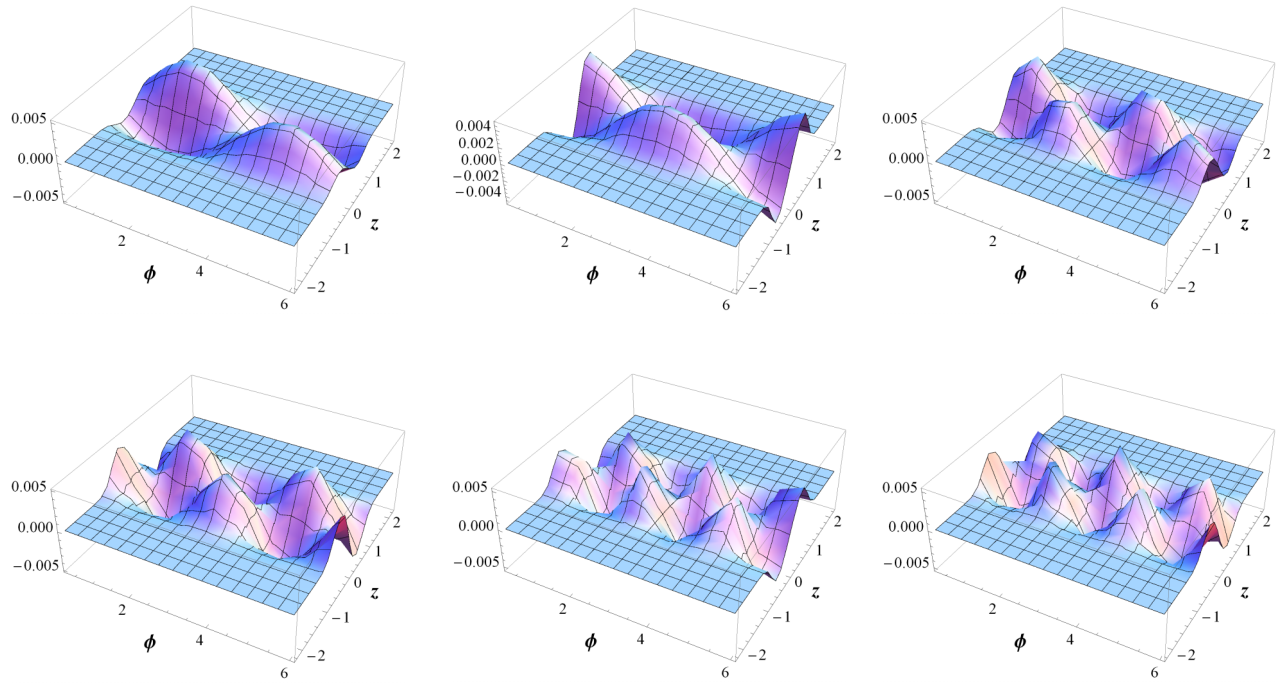

FIG. 4. 2D (ϕ, z) cuts of the 9D vibrational wavefunctions of the computed combination bands of torsion with "proton-hopping" and dissociation for H_5^+ (and D_5^+); first row: ($\nu_{PH}+\nu_{TE}$, $\nu_{PH}+\nu_{TO}$, $\nu_{PH}+2\nu_{TE}$), second row: ($\nu_{PH}+2\nu_{TO}$, $\nu_{PH}+3\nu_{TE}$, $\nu_{PH}+3\nu_{TO}$).

of the bending-type eigenstates and their quasi-degenerate nature is unexpected.

Third, it can also be observed that for H_5^+ and D_5^+, and also for some of the other isotopomers, after the first four bending-type states there is no description pattern for the rest of the states which could be applied throughout the isotopomers. The standard rules fail in these cases since not all possible combination bands are "observable." The wavefunction is often a strong mixture of different states, which results in complicated, sometimes recurring labels. Comparison of different 2D cuts of the wavefunctions yields, in some cases, contradictions. The elaborate and delicate mixings observed, see Figure S4 of the supplementary material[47] for an example, makes the labeling rather difficult.

It is also notable that the dissociative motion of the molecule, corresponding to ν_D, which by default can favor the left as well as the right sides, picks only one of the sides, resulting in the $\nu_{D_{(-)}}$ and $\nu_{D_{(+)}}$ labels (see, e.g., Figure S4 of the supplementary material[47] for the 36th energy level of H_5^+, which is assigned as $\nu_{\theta_1}+\nu_{D_{(-)}}+2\nu_{TO}$).

When going higher in energy, the θ_1 and the x labels, as well as θ_2 and y, appear both separately and in combination. The bending overtones, $2\nu_{\theta_1}$, $2\nu_{\theta_2}$, $2\nu_x$, and $2\nu_y$, or $2(\nu_{\theta_1}+\nu_x)$ and $2(\nu_{\theta_2}-\nu_y)$ as more appropriately labeled, do not appear among the first 50 energy levels, except one for $[D_2-D-H_2]^+$. Instead of the expected behavior, there are several combinations of these bending-type motions with ν_D, ν_{PH}, and ν_T.

The combination bands, especially when the torsion is included, are even less defined. Some fundamentals, e.g., $(\nu_{\theta_1}-\nu_x)$ and $(\nu_{\theta_2}+\nu_y)$ for H_5^+, as well as some basic combination bands, are missing (e.g., not all of the combination bands of the first four bending states with ν_{PH} can be assigned), while more complicated combination bands appear. Most of the missing states are connected to the torsional motion. In some cases it cannot be decided if ν_{TE} or ν_{TO} is part of the label; furthermore, whether ν_T or $2\nu_T$ should be assigned. In conclusion, it seems that higher in energy the torsional motion almost freely combines with most other vibrational motions. It is also remarkable that the eigenvalues of these bending-type states cannot be estimated by simply adding the eigenvalues of the participating fundamentals.

While for set I the eigenenergies corresponding to the XBB PES are smaller than their ABPDVR counterparts, the corresponding differences for the set II bend-only states are all negative, which means that the XBB PES results in larger eigenvalues. Higher in energy, when the ν_D label also appears in the assignment, the wavenumbers become smaller again with the XBB PES. For D_5^+, all the computed wavenumber differences are negative, the XBB values being larger (see Table V).

Finally, we note that the energies of the vibrational states belonging to set II motions seem to be less converged, as well. Increasing the size of the basis along the θ_1, θ_2, x, and y coordinates using the same coordinate intervals, resulting in a Hamiltonian matrix of size 1000M, occasionally yields several cm^{-1} changes.

C. Vibrational states of $H_{5-n}D_n^+$ (n = 1, 2, 3, and 4)

There are some general findings characterizing the vibrational states of all $H_{5-n}D_n^+$, n = 1–4, isotopomers. These are discussed first: (1) The splitting of the ν_{TE} and ν_{TO} vibrational states does not depend on whether H or D is the middle atom; the splitting only depends on the identity of the two sides. To wit, for the H_2–H_2, HD–H_2, H_2–D_2, HD–HD,

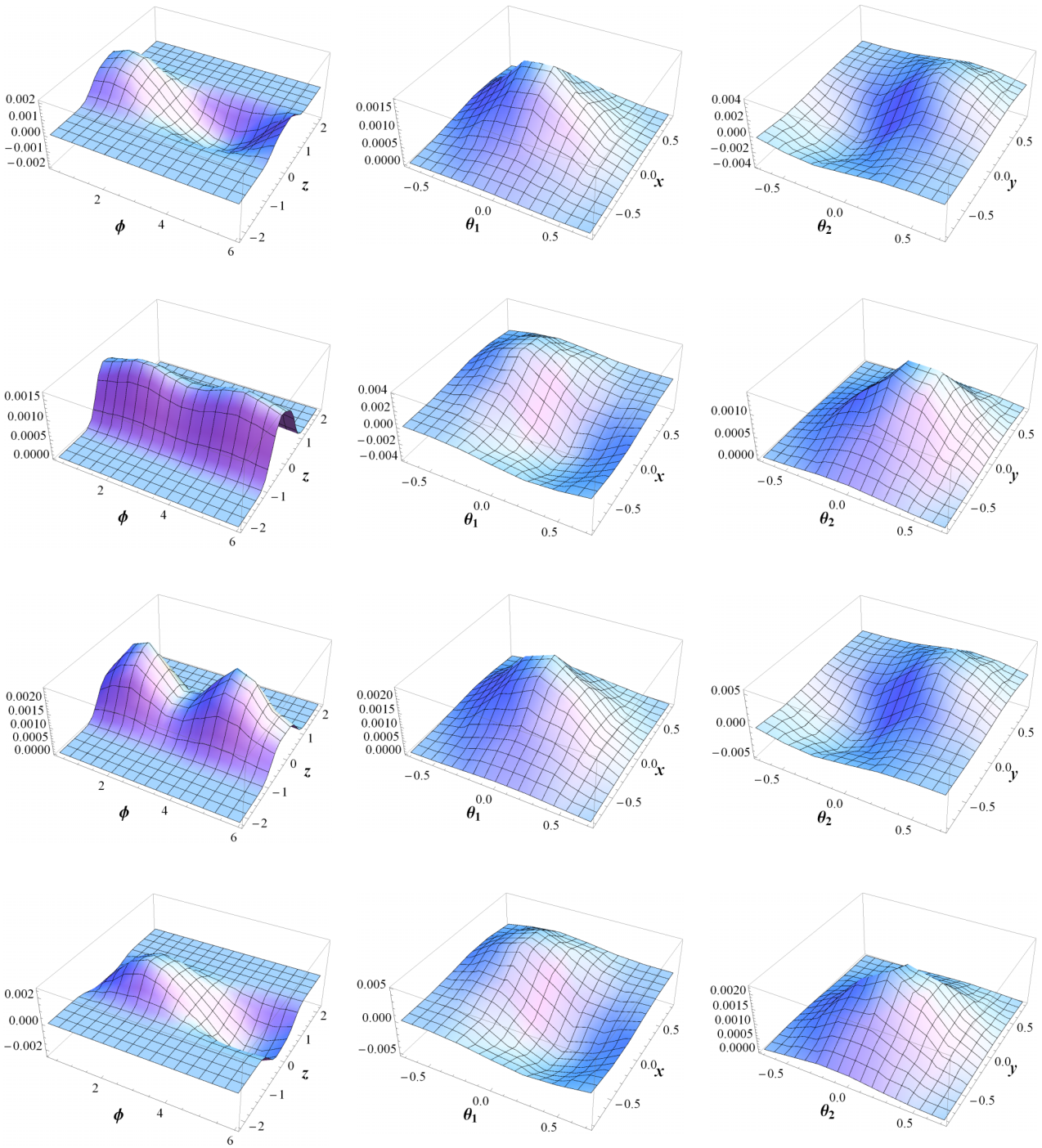

FIG. 5. 2D (ϕ, z; θ_1, x; θ_2, y) cuts of the 9D vibrational wave functions of the computed bending type eigenstates of H_5^+ (12th, 13th, 16th, 17th) and D_5^+ (16th–19th), $\nu_{\theta_2}-\nu_y+\nu_{\mathrm{TE}}$, $\nu_{\theta_1}+\nu_x$, $\nu_{\theta_2}-\nu_y$, and $\nu_{\theta_1}+\nu_x+\nu_{\mathrm{TE}}$, respectively. For θ_1 and θ_2 the cosines of the angles mentioned are the effectively used bending coordinates.

HD–D_2, and D_2–D_2 cases the $\nu_{\mathrm{TE}}/\nu_{\mathrm{TO}}$ values, in cm^{-1}, are 90/136, 76/122, 64/109, 62/107, 48/94, and 36/81, respectively (note also the almost constant 14 cm^{-1} decrease per a D substitution in this set of values). As can also be seen, the splitting of the ν_{TE} and ν_{TO} states is basically constant among the isotopomers, it is always about 46 cm^{-1}. (2) In clear contrast, the $2\nu_{\mathrm{TE}} - 2\nu_{\mathrm{TO}}$ splitting changes from isotopomer to isotopomer, its value is 0.7 cm^{-1} in H_5^+, 3.2 cm^{-1} in D_5^+, 0.4 cm^{-1} for H_4D^+, and 3.1 cm^{-1} for HD_4^+. Apart from possible convergence problems it is not clear how to explain the different "behavior" of the ν_{T} and $2\nu_{\mathrm{T}}$ states. (3) The hopping mode is sensitive to the quality of the middle atom but more or less independent of the sides. (4) The torsional progression $n\nu_2$, $n = 1,2,3,4$, observed here has been noted and explained in Ref. 8. The simple k^2 dependence of $n\nu_2$ holds for all isotopomers.

Next, the vibrational states of the "symmetric" and "quasi-symmetric" isotopomers are discussed, i.e., those with homonuclear diatomics at the sides (see Tables VII and VIII). Substituting the middle atom of H_5^+ or D_5^+ results in

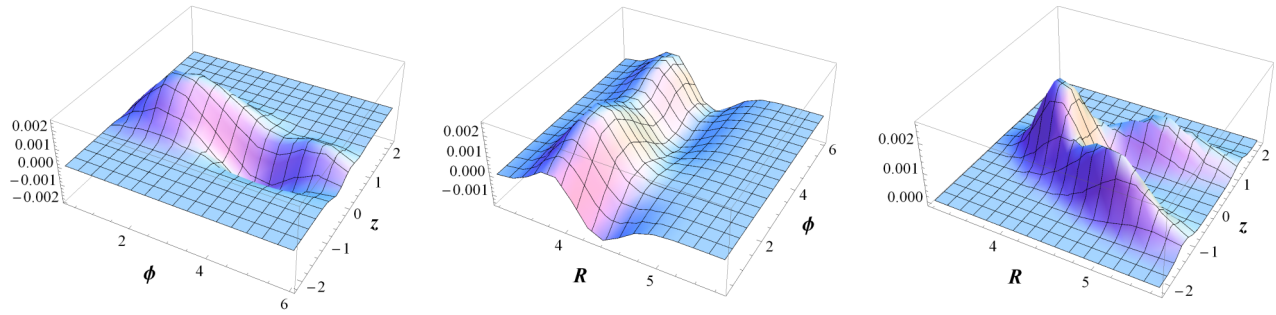

FIG. 6. Different 2D cuts of the 9D vibrational wavefunctions of the 33rd eigenstate of $[DH–D–DH]^+$ (877.8 cm^{-1}), with a viable label of $(\nu_{\theta_1}-\nu_x)-(\nu_{\theta_2}+\nu_y)+\nu_{TE}$. Note that information contained in the 2D (ϕ, z), 2D (R, ϕ), and 2D (R, z) plots is contradictory.

the $[H_2–D–H_2]^+$ and $[D_2–H–D_2]^+$ isotopomers, respectively. These isotopomers basically have the same symmetry as H_5^+ and D_5^+. One can enlarge this set by the $[D_2–H–H_2]^+$ and $[D_2–D–H_2]^+$ isotopomers, whereby the two sides are different but there are homonuclear diatomics on the sides. The energy level structure of these four isotopomers is very similar to those of H_5^+ or D_5^+.

The first group of vibrational states, characterized by the ν_{TE}, ν_{PH}, and ν_D labels, has, similarly to H_5^+, no mixing with bending-type motions. Putting D in the middle decreases the wavenumber of the motions of ν_{PH} and ν_D, while the D_2 unit on the side decreases the torsional frequency. Since the wavenumber of the torsion decreases more than the other two motions, $[D_2–H–D_2]^+$ and $[H_2–D–H_2]^+$ have the highest and lowest number of states belonging to this group.

Characterization of the remaining states cannot be done uniformly. Since $[H_2–D–H_2]^+$ and $[D_2–H–D_2]^+$ appear to have the same "symmetry" as H_5^+, the peculiar quasi-degeneracy of the first four bending levels appears to be the same as for H_5^+. The two outer D_2 units decrease the wavenumbers more than the internal D. It is also notable that in the low-energy region, after the first four levels, the bending states combine with ν_{PH} for $[H_2–D–H_2]^+$ and with ν_{TE} for $[D_2–H–D_2]^+$, due to the position of the D(s) in the molecule. The general findings

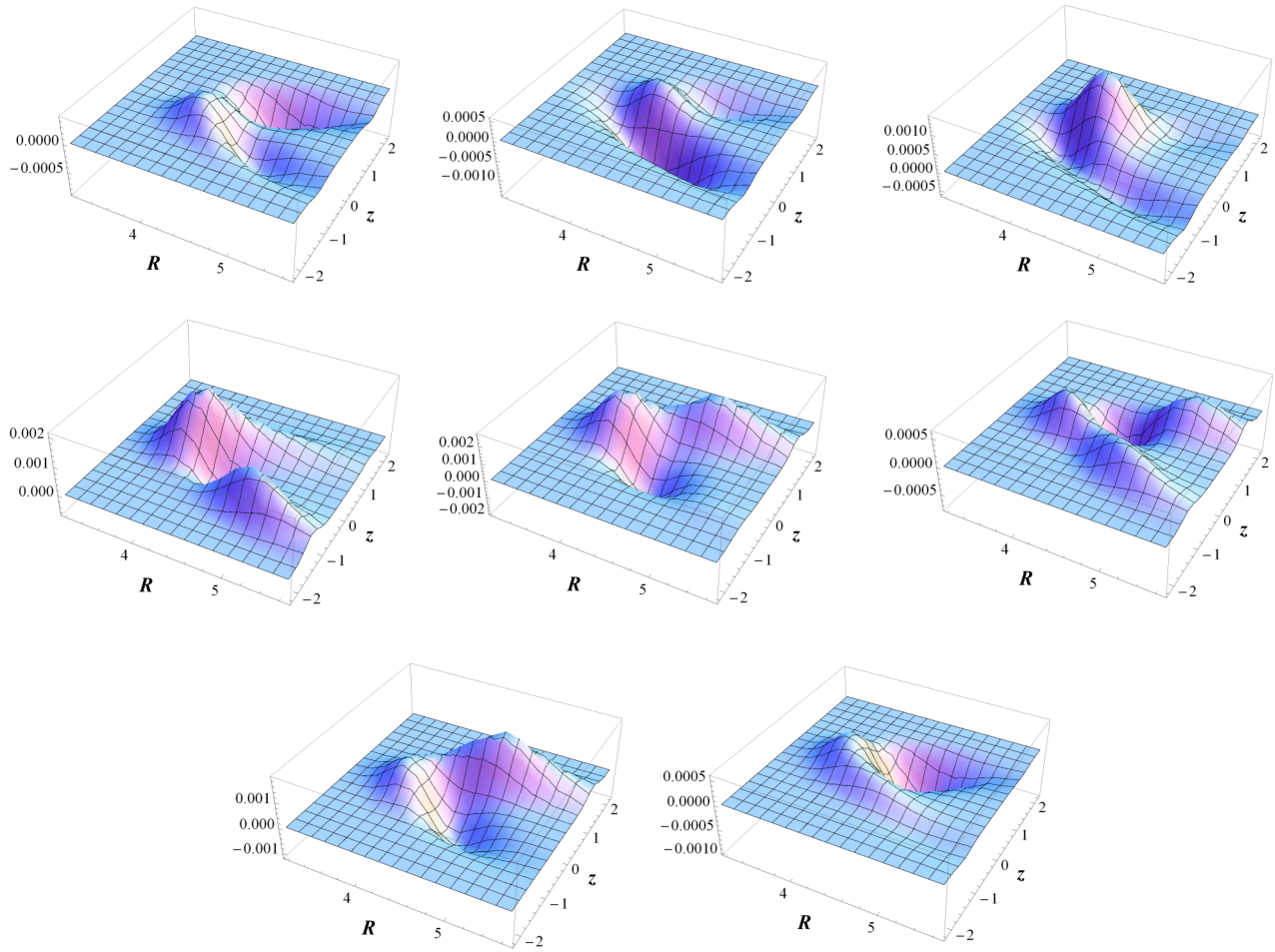

FIG. 7. 2D (R, z) cuts of the 9D vibrational wavefunctions of the 29th, 30th, 35th, 37th, 41st, 45th, 47th, 48th eigenstates of $[DH–H–DH]^+$, an isotopomer of $H_3D_2^+$. The structure of the wavefunctions is unusual for these eigenstates.

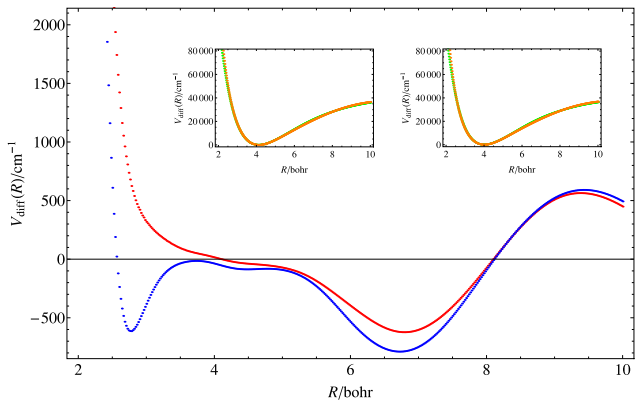

FIG. 8. The difference of the two PESs employed in this study, $V_{\rm diff} = V({\rm XBB}) - V({\rm ABPDVR})$, along the R coordinate. The values of the other coordinates are either frozen (see Table I for details) to the C_{2v} global minimum (red curve) or to the D_{2d} transition state (blue curve). The insets, with the ABPDVR and XBB PESs plotted in green and orange, respectively, show the actual values of the PESs, corresponding to the C_{2v} (left) and D_{2d} (right) structures, respectively.

detailed above for the set II states of H_5^+, i.e., the somewhat chaotic behavior of such states, are applicable here, as well.

Since the $[D_2–H–H_2]^+$ and $[D_2–D–H_2]^+$ isotopomers are different but symmetric on the two sides, the energy level structure changes only slightly for these species. Although the degeneracy of the first four states disappears, the peculiar order of the $(\nu_{\theta_2} - \nu_y) + \nu_{\rm TE}$ and $(\nu_{\theta_2} - \nu_y)$ states remains.

Finally, the energy-level structure of the non-symmetric isotopomers is discussed. The remaining six isotopomers have a common trait: all of them have at least one outer HD unit. Although at first $[DH–H–DH]^+$ and $[DH–D–DH]^+$ appear to be "symmetric," the wavefunctions of the eigenstates suggest that they should be handled separately from the other six isotopomers. The most important difference of this group from the other two is that the higher-lying eigenstates of the R, ϕ, z group cannot be assigned purely with the $\nu_{\rm TE}$, $\nu_{\rm PH}$, and $\nu_{\rm D}$ labels. Although the first 10 states are pure non-bending, the next ones typically mix considerably with the bending states (see Table IX). We should also note that for these isotopomers some of the unique labels of the first two groups appear multiple times. This is unusual for semirigid molecules but seemingly it happens quite a few times for the astructural molecules studied here, where mixing is particularly strong.

The bending energy levels of these six isotopomers, especially of the seemingly symmetric $[DH–H–DH]^+$ and $[DH–D–DH]^+$, seem to show a more chaotic dynamic behavior than the other isotopomers, as judged by the 2D wavefunction cuts. There are no real fundamentals, every bending-type state, even at low energy, displays a rather complex combination of the possible motions. In several cases not only are the 2D bending wavefunction plots in contradiction with each other (see Figure 6 and S4 of the supplementary material[47]), but also the wavefunction plots corresponding to the first set of coordinates mimic this behavior (see Fig. 7), which results in a difficult labeling procedure. Despite the primarily bending character of these states, especially for $[DH–H–DH]^+$ and $[DH–D–DH]^+$, the chaotic mixing can result in very unique structures in the 2D (R, z) wavefunction cuts (see Fig. 7), mixing the motions of the two coordinate sets.

VI. SUMMARY

The vibrational energy level structure of the $H_{5-n}D_n^+$, n = 0–5, deuterated H_5^+ isotopologues is studied up to about half of the first dissociation energy. The variational nuclear-motion computations performed confirm that the six possible isotopologues form 12 isotopomers, one for n = 0 and 5, two for n = 1 and 4, and three for n = 2 and 3. This simplification is due to the fact that of the three large-amplitude motions of H_5^+, proton hopping (PH), torsion (T), and scrambling (SC), only the scrambling motion has a large enough barrier to prevent facile exchange of the atoms involved. This unfeasible permutation lowers the apparent symmetry of the systems.

It is true for all isotopologues that the isotopomer with H in the middle has a considerably lower ZPVE, and thus a considerably higher stability, than when D is the middle atom. As a second rule governing stability, a more stable isotopomer results if the sides form homonuclear diatomics.

The mostly benchmark-quality vibrational energies obtained during the present study prove that, especially at higher energies, the previously computed DMC and MCTDH vibrational energies suffer from certain approximations. It is suggested that during MCTDH computations of energy levels for difficult, astructural molecules, like those of the present study, special care must be taken to ensure that the computation yields precise energy levels, correctly representing the original PES.

The computation of the vibrational eigenstates of the 12 isotopomers utilized two distinct global PESs.[20,21] The present study proves that the use of the two PESs results in very similar eigenstates, the only significant difference is in the description of the dissociative (D) motion. This conclusion is somewhat different from what previous DMC and MCTDH studies suggested.

Most of the time the two-dimensional wavefunction cuts proved to be highly useful to interpret the computed wavefunctions and assign labels for them. The labeling process proved to be straightforward for motions involving the ϕ, z, and R coordinates, corresponding to the T, PH, and D motions, respectively. However, the vibrational eigenstates corresponding to bending-type motions show significant mixing and more unusual structure. It does not seem to be true that, at least in the energy region studied, an H → D substitution changes considerably the characteristics of the vibrational eigenstates.

Overall, it seems that the energy-level characteristics of the astructural $H_{5-n}D_n^+$ molecules warrant further elaborate studies utilizing several advanced techniques of nuclear-motion theory if we were to understand the complex dynamics characterizing these molecules up to the first dissociation limit and beyond. For the higher-energy states involving the excited scrambling motion the apparent symmetry is expected to change, adding further complication to the understanding of the intriguing rovibrational dynamics of these systems.

ACKNOWLEDGMENTS

The present work received support from the Hungarian Scientific Research Fund (OTKA, Grant No. NK83583) and from the COST action MOLIM (No. CM1405, Molecules in Motion). The authors are grateful to Professor Anne McCoy for several discussions related to the determination of the ZPVEs by the DMC technique. We thank the help of Dr. C. Fábri with the GENIUSH computations. A.G.C. is also grateful for illuminating discussions with Dr. Rita Prosmiti and Dr. Octavio Roncero concerning details of their computations on the H_5^+ system.

[1]E. B. Wilson, J. C. Decious, and P. C. Cross, *Molecular Vibrations* (McGraw-Hill, New York, 1955).
[2]H. W. Kroto, *Molecular Rotation Spectra* (Dover, New York, 1992).
[3]A. G. Császár, C. Fábri, T. Szidarovszky, E. Mátyus, T. Furtenbacher, and G. Czakó, Phys. Chem. Chem. Phys. **14**, 1085 (2012).
[4]I. M. Mills and H. W. Thompson, Proc. R. Soc. A **226**, 306 (1954).
[5]P. R. Bunker and H. C. Longuet-Higgins, Proc. R. Soc. A **280**, 340 (1964).
[6]C. di Lauro, P. R. Bunker, J. W. C. Johns, and A. R. W. McKellar, J. Mol. Spectrosc. **184**, 177 (1997).
[7]C. Fábri, J. Sarka, and A. G. Császár, J. Chem. Phys. **140**, 051101 (2014).
[8]J. Sarka, C. Fábri, T. Szidarovszky, A. G. Császár, Z. Lin, and A. B. McCoy, Mol. Phys. **113**, 1873 (2015).
[9]H. Schmiedt, S. Schlemmer, and P. Jensen, J. Chem. Phys. **143**, 154302 (2015).
[10]R. Wodraszka and U. Manthe, J. Phys. Chem. Lett. **6**, 4229 (2015).
[11]W. Paul, B. Lücke, S. Schlemmer, and D. Gerlich, Int. J. Mass Spectrom. Ion Processes **149-150**, 373 (1995).
[12]W. Paul, S. Schlemmer, B. Lücke, and D. Gerlich, Chem. Phys. **209**, 265 (1996).
[13]R. Prosmiti, P. Villarreal, and G. Delgado-Barrio, J. Phys. Chem. A **107**, 4768 (2003).
[14]M. Pavanello, L. Adamowicz, A. Alijah, N. F. Zobov, I. I. Mizus, O. L. Polyansky, J. Tennyson, T. Szidarovszky, A. G. Császár, M. Berg, A. Petrignani, and A. Wolf, Phys. Rev. Lett. **108**, 023002 (2012).
[15]O. L. Polyansky, A. Alijah, N. F. Zobov, I. I. Mizus, R. I. Ovsyannikov, J. Tennyson, L. Lodi, T. Szidarovszky, and A. G. Császár, Philos. Trans. R. Soc., A **370**, 5014 (2012).
[16]D. Lauvergnat and A. Nauts, J. Chem. Phys. **116**, 8560 (2002).
[17]S. N. Yurchenko, W. Thiel, and P. Jensen, J. Mol. Spectrosc. **245**, 126 (2007).
[18]J. M. Bowman, T. Carrington, and H. Meyer, Mol. Phys. **48**, 2145 (2008).
[19]Y. Yamaguchi, J. F. Gaw, R. B. Remington, and H. F. Schaefer III, J. Chem. Phys. **86**, 5072 (1987).
[20]Z. Xie, B. J. Braams, and J. M. Bowman, J. Chem. Phys. **122**, 224307 (2005).
[21]A. Aguado, P. Barragán, R. Prosmiti, G. Delgado-Barrio, P. Villarreal, and O. Roncero, J. Chem. Phys. **133**, 024306 (2010).
[22]A. Aguado, C. Sanz-Sanz, P. Villareal, and O. Roncero, Phys. Rev. A **85**, 032514 (2012).
[23]P. H. Acioli, Z. Xie, B. J. Braams, and J. M. Bowman, J. Chem. Phys. **128**, 104318 (2008).
[24]R. P. de Tudela, P. Barragán, R. Prosmiti, P. Villarreal, and G. Delgado-Barrio, J. Phys. Chem. A **115**, 2483 (2011).
[25]P. Barragán, R. P. de Tudela, R. Prosmiti, P. Villarreal, and G. Delgado-Barrio, Phys. Scr. **84**, 028109 (2011).
[26]B. A. McGuire, Y. Wang, J. M. Bowman, and S. L. Widicus Weaver, J. Phys. Chem. Lett. **2**, 1405 (2011).
[27]Á. Valdés, R. Prosmiti, and G. Delgado-Barrio, J. Chem. Phys. **136**, 104302 (2012).
[28]Á. Valdés, R. Prosmiti, and G. Delgado-Barrio, J. Chem. Phys. **137**, 214308 (2012).
[29]Z. Lin and A. B. McCoy, J. Phys. Chem. Lett. **3**, 3690 (2012).
[30]Z. Lin and A. B. McCoy, J. Phys. Chem. A **117**, 11725 (2013).
[31]H. Song, S.-Y. Lee, M. Yang, and Y. Lu, J. Chem. Phys. **138**, 124309 (2013).
[32]Á. Valdés and R. Prosmiti, J. Phys. Chem. A **117**, 9518 (2013).
[33]Á. Valdés and R. Prosmiti, Phys. Chem. Chem. Phys. **16**, 6217 (2014).
[34]Z. Lin and A. B. McCoy, J. Chem. Phys. **140**, 114305 (2014).
[35]M. L. Marlett, Z. Lin, and A. B. McCoy, J. Phys. Chem. A **119**, 9405 (2015).
[36]Z. Lin and A. B. McCoy, J. Phys. Chem. A **119**, 12109 (2015).
[37]T. C. Cheng, B. Bandyipadyay, Y. Wang, S. Carter, B. J. Braams, J. M. Bowman, and M. A. Duncan, J. Phys. Chem. Lett. **1**, 758 (2010).
[38]T. C. Cheng, L. Jiang, K. R. Asmis, Y. Wang, J. M. Bowman, A. M. Ricks, and M. A. Duncan, J. Phys. Chem. Lett. **3**, 3160 (2012).
[39]J. Demaison, A. G. Császár, I. Kleiner, and H. Mollendal, J. Phys. Chem. A **111**, 2574 (2007).
[40]H.-D. Meyer, U. Manthe, and L. S. Cederbaum, Chem. Phys. Lett. **165**, 73 (1990).
[41]E. Mátyus, G. Czakó, and A. G. Császár, J. Chem. Phys. **130**, 134112 (2009).
[42]C. Fábri, E. Mátyus, and A. G. Császár, J. Chem. Phys. **134**, 074105 (2011).
[43]C. Fábri, E. Mátyus, and A. G. Császár, Spectrochim. Acta, Part A **119**, 84 (2014).
[44]J. C. Light and T. Carrington, Jr., Adv. Chem. Phys. **114**, 263 (2000).
[45]C. Lanczos, J. Res. Natl. Bur. Stand. **45**, 255 (1950).
[46]See http://iopenshell.usc.edu/downloads/ezpes/ for "iopenshell webpage" (last accessed October 16, 2015).
[47]See supplementary material at http://dx.doi.org/10.1063/1.4946808 for additional information regarding (I) details on the parameters of the two PESs applied; (II) the ABPDVR PES along the z coordinate; (III) comparison of the two PESs along the z coordinate; (IV) all of the computed vibrational energy levels for H_5^+ and all of its deuterated isotopologues and isotopomers; and (V) figures with 2D plots of the wavefunctions.
[48]J. Echave and D. C. Clary, Chem. Phys. Lett. **190**, 225 (1992).
[49]H. Wei and T. Carrington, Jr., J. Chem. Phys. **97**, 3029 (1992).
[50]V. Szalay, G. Czakó, A. Nagy, T. Furtenbacher, and A. G. Császár, J. Chem. Phys. **119**, 10512 (2003).